Electro-deposition Assisted Synthesis of Cu/MoS_2 Nanostructures for Efficient Hydrogen Evolution Reaction

SurraYonasTerfa

A thesis Submitted to Department of Applied Chemistry,

School of Applied Natural Science

Presented in Partial Fulfillment of the Requirement for the Degree of Master's in Applied Chemistry (Physical Chemistry)

Office of Graduate Studies

Adama Science and Technology University

February, 2024

Adama, Ethiopia

Electro-deposition Assisted Synthesis of Cu /MoS_2Nanostructures for Efficient Hydrogen Evolution Reaction

Surra Yonas Terfa

Major advisor: BedasaAbdisa (Ph.D.)

Co-Advisor: Lemma Teshome(Ph.D.)

A thesis Submitted to Department of Applied Chemistry

School of Applied Natural Science

Presented in Partial Fulfillment of the Requirement for the Degree of Master's in Applied Chemistry (Physical Chemistry)

Office of Graduate Studies

Adama Science and Technology University

February, 2024

Adama, Ethiopia

Declaration

I declare that this thesis entitled "Electro-deposition Assisted Synthesis of Cu/MoS_2 Nanostructures for Efficient Hydrogen Evolution Reaction" is my own work and has not been submitted to any university for similar purpose. The references used in this thesis are duly recognized by proper citations.

Surra Yonas Terfa _____ _____

Name of student Signature Date

Recommendation of Advisors

We, the advisors of this thesis work, hereby certify that we have closely advised the student while developing the proposal and read the draft thesis work entitled **"Electro-deposition Assisted Synthesis of Cu/MoS_2 Nanostructures for Efficient Hydrogen Evolution Reaction"** prepared under our guidance by Surra Yonas. Therefore, we recommend the submission of the thesis work to the department for further review and evaluation.

Bedasa Abdisa(Ph.D.)	_____	_____
Major Advisor	Signature	Date
Lemma Teshome(Ph.D.)	_____	_____
Co-advisor	Signature	Date

Thesis Approval Sheet

We here by certify that the recommendation and suggestion given by the thesis review committee are appropriately incorporated into the final thesis entitled "**Electric Field-Assisted Synthesis of Cu/MoS_2 Nanostructures for Efficient Hydrogen Evolution Reaction"** by Surra Yonas.

Bedasa Abdisa (Ph.D.)	_____	_____
Major Advisor	Signature	Date
Lemma Teshome(Ph.D.)	_____	_____
Co-advisor	Signature	Date

We, the undersigned, members of the Board of Reviewers of the thesis open defense by SurraYonas have read and evaluated the thesis entitled **"Electro-deposition Assisted Synthesis of Cu/MoS_2 Nanostructures for Efficient Hydrogen Evolution Reaction"** and assessed the understanding of the candidate about the research work . This is, therefore, to certify that the thesis is accepted and we recommend the implementation of this thesis.

Defaru Negara (Ph.D.)	_____	_____
Chairperson	Signature	Date
Fedilu Kedir (Ph.D.)	_____	_____
Internal Examiner	Signature	Date
Endale Tsegaye (Ph.D.)	_____	_____
External Examiner	Signature	Date

Final approval and acceptance of the thesis is contingent upon submission of its final copy to the Office of Postgraduate Studies (OPGS) through the Department Graduate Council (DGC) and School Graduate Committee (SGC).

_____	_____	_____
Department Head	Signature	Date
_____	_____	_____
School Dean	Signature	Date
_____	_____	_____
Office of Postgraduate Studies, Dean	Signature	Date

ACKNOWLEDGEMENTS

First and foremost, I would like to thank Almighty God for giving me strength, knowledge, and ability.

Next, I would like to express my deepest gratitude to my family for giving me freedom, financial support and encouragement in my life.

In addition, I would like to express my deepest gratitude to my advisors, Bedassa Abdissa (Ph.D.) and Lemma Teshome (Ph.D.), for their patience, fruitful advice, and friendly approach during the whole period of doing project, and I would like to further express my deepest gratitude to my co-advisor, Lemma Teshome (Ph.D.), for his professional, very invaluable, unreserved advice and guidance and material and chemical support.

Furthermore, I would like to express my sincere gratitude to all academic, technical, and support staff of the Department of Applied Chemistry, Applied Biology, and Material Science at Adama Science and Technology University, for providing the necessary assistance and facilities to conduct my research work.

Lastly, I would like to express my deepest gratitude to AkaluTerfa (Ph.D.) for his ideal support.

Table Content

Content

LIST OF ACRONYM AND ABBREVIATION

2D	Two-dimensional
AFM	Atomic Force Microscope
C_{dl}	Double-layer Capacitances
CE	Counter Electrode
CFC	Carbon Fiber Cloth
CVs	Cyclic Voltammograms
DFT	Density Functional Theory
ECSA	Electrochemical Active Surface Area
EDS	Energy-Dispersive X-Ray Spectroscopy
FTO	Fluorine Doped Tin Oxide
EIS	Electrochemical Impedance Spectroscopy
HER	Hydrogen Evolution Reaction
LSVs	Linear Sweep Voltammograms
RHE	Reversible Hydrogen Electrode
SCE	Saturated Calomel Electrode
SEM	Scanning Electron Microscope
TEM	Transmission Electron Microscopy
V_{op}	Overall Operational Voltage
XPS	X-ray Photoelectron Spectroscopy
XRD	X-ray Diffraction

LIST OF TABLE

LIST OF FIGURE

Abstract

To replace Pt-based compounds in the electrocatalytic hydrogen evolution reaction (HER),MoS_2 has already been established as an efficient catalyst. The electrocatalytic activity of MoS_2 is further improved the morphology and the electronic structure through coating, which helps the band energy position to be modified .Presently, Cu/MoS_2nanostructure is synthesized via electrodeposition technique.The synthesized Cu/MoS_2nanostructure were characterized using various analytical techniques, including X-ray diffraction, scanning electron microscopy, and energy dispersive X-ray spectroscopy. The results indicate that the coating of MoS_2 by Cu metal is leads to the formation of highly crystalline Cu/MoS_2 nanostructure with a well-defined interface.The electrochemical properties of the Cu/MoS_2 nanomaterial were evaluated using linear sweep voltammetry, cyclic voltammetry and Electrochemical impedance spectroscopy. The optimized Cu/MoS_2 nanostructure which exhibit low overpotential of -149 mV and a Tafel slope of 117 mV/dec, indicating superior catalytic activity compared to bare MoS_2. This study provides combining Cu with MoS_2 could potentially improve the HER performance and conductivity, which can have significant implications for renewable energy applications.

Keywords: *Electrodeposition, Hydrogen Evolution Reactions, Catalytic Activity, Molybdenum disulfide and Nanostructure.*

CHAPTER ONE

1. INTRODUCTION

1.1 Background of the study

Sustainable development of society is closely linked to two critical concerns: energy and the environment. To date, fossil fuels - including natural gas, oil, and coal - have been considered the primary energy source, meeting approximately 85% of the world's energy demand. However, burning of fossil fuels, results in the release of greenhouse gases (such as CO_2, SO_x, and NO_x) (Samantara & Ratha, 2019). Studies conducted in this field have brought attention to the possibility of hydrogen being a suitable substitute for fossil fuels(Alonso-Vante et al., 2019). Free hydrogen does not exist abundantly and is mainly present in compounds like hydrocarbons and water (Tiwari et al., 2018).Three distinct pathways are utilized for hydrogen production:(1) steam methane reforming, (2) coal gasification, and (3)water electrolysis (Alonso-Vante et al., 2019).Water electrolysis is an eco-friendly method for producing renewable hydrogen. This electrochemical process involves the anodic generation of O_2, known as the "oxygen evolution reaction", and the cathodic generation of H_2, known as the "hydrogen evolution reaction" (Herbaut et al., 2021). The hydrogen and oxygen evolution reactions happen only when a specific thermodynamic potential is reached:0.00 V and 1.23 V for hydrogen generation (HER) and oxygen generation (OER) (vs. RHE), respectively (Briefs & Materials, 2018).In practical applications, water electrolysis typically requires a higher voltage than the thermodynamic potential to overcome unfavorable factors like high overpotential and sluggish kinetics(Bhat & Nagaraja, 2021). As a result, energy researchers are primarily focused on reducing overpotential by enhancing electrodes, electrocatalysts, and electrolytes, or by gaining further knowledge about the kinetics of electrode reactions(Samantara & Ratha, 2019).

During the HER, the advanced electrocatalyst is a key component that reduces the overpotential of electrodes to be low, producing a high current density and consequently increasing the yield of this important electrochemical process(J. Cao et al., 2017a) .Thus far, electrocatalysts that utilize precious metals like platinum and palladium have exhibited considerable potential. Nevertheless, their extensive expense and scarcity have impeded their broad implementation(Pataniya & Sumesh, 2022). As a result, the majority of research

has been focused on developing electrocatalysts that are sourced from abundant and non-preciousmaterialswhile still retaining exceptional electrocatalytic activity(Ilyas, Raziq et al, 2021).Earth-abundant transition-metal dichalcogenides (TMDs) with a general formula of MX_2 (M = transition metal; X = chalcogen), including two-dimensional (2D) layered materials like MoS_2, WS_2, $MoSe_2$, WSe_2, TaS_2, and TiS_2, have gained considerable attention in the field of electrocatalysis owing to their fascinating chemical and electronic features(F. Wang et al., 2015).MoS_2nanosheets have garnered considerable attention in the field of electrocatalysis among TMDs, primarily because of their S-edges, which have an optimal Gibbs free energy of hydrogen adsorption(ΔGH*) of 0.06 eV.This implies that the active sites of MoS_2 are situated at the edges with an energy level that is nearly 0 eV(Sun & Meng, 2021).

In 2005, Jens Nørskov's research group investigated the mechanism of HER on various catalysts utilizing density functional theory (DFT) calculations. Their findings revealed that the Gibbs free energy (ΔG) of MoS_2 nanoparticles for HER is similar to that of Pt, indicating MoS_2's potential for HER. Furthermore, subsequent experiments confirmed that the edge of MoS_2nanosheets is electrochemically active(F. Wang et al., 2015).Experimental and theoretical findings have also suggested that the active sites of MoS_2, located at the basal planes, are usually catalytically inactive(Y. Li et al., 2011). However due to their high surface energy and interlayer van der Waals interactions, MoS_2 nanostructures tend to stack together, resulting in limited active sites and hindered electron transport. As a result, the low electrical conductivity and restricted active edges of MoS_2 have limited its broader application(Sharma et al., 2021). To overcome these problems, the couplings of two or more material components to produce heterostructures catalysts with rich interfaces have recently drawn attention of many researchers in this area(Sun & Meng, 2021).

A volcano plotwas generated to depict the relationship between the exchange current density,Cu has a slightly lower exchange current density than the noble Pt-group metals(F. Li, Zhang, et al., 2015). Thus, combining Cu with MoS_2 could potentially improve the HER performance and conductivity(J. Cao et al., 2017b). Incorporating Cu into the MoS_2 catalyst substantially increases the catalytic efficiency of HER(Gudal et al., 2022). The MoS_2/Cu electrocatalyst exhibits excellent electrocatalytic activity and high stability in acidic solutions, as evidenced by a good Tafel slope of approximately 75.8 mV dec^{-1}(Ilyas, et. al 2021).Therefore, this work presents Cu/MoS_2nanostructure catalyst synthesized by two step

electrodeposition method as an excellent electrocatalytic activity and high stability material in the alkaline solution for HER.

1.2 Statement of the Problem

The practical application of MoS_2-based catalysts for the hydrogen evolution reaction (HER) is limited by the high overpotential required which is a result of limited active sites on the surface of MoS_2 and its low electrical conductivity. To address this limitation, the coupling of two or more components can be used to produce heterostructures with rich interfaces. The construction of heterostructures can regulate the interface electronic structure and trigger charge-transfer kinetics which can improve the catalytic performance of materials (Sun & Meng, 2021). In this work, Cu-based nanomaterials was chosen for the heterostructure with MoS_2 due to their important properties including a Gibbs free energy of adsorbed atomic hydrogen that lies below those of the noble Pt-group metals, high earth abundance, low-cost of transition metals, nontoxicity, and ease of preparation.

1.3. Objectives of the Study

1.3.1. General Objective

The main objective of this work was to synthesize Cu/MoS_2 nanostructures using electrodeposition assisted method and study its electrocatalytic performance for hydrogen generation reaction.

1.3.2. Specific Objectives

The specific objectives of this study were:

i. To synthesize Cu/MoS_2nanomaterials by electrochemical deposition method.
ii. To characterize the synthesized Cu/MoS_2 nanomaterial using XRD, SEM, EDS, TEM, HRTEM and SAED techniques.
iii. To probe the electrochemical performance of Cu/MoS_2 towards HER.
iv. Compare the HER performance of the Cu/MoS_2 Nanostructure electrocatalyst with that of single MoS_2.

1.4. Significance of the Study

This study is significant for sustainable energy production as it focuses on developing efficient and sustainable methods for hydrogen gas production through electrochemical hydrogen evolution. By addressing current electrocatalysts limitations and proposing innovative solutions, this research contributes to the transition towards a clean and renewable energy future, diminishing dependence on fossil fuels and mitigating environmental consequences. Additionally, the study tackles economic challenges associated with large-scale hydrogen production by exploring alternative catalyst materials and design strategies, intending to reduce expenses and enhance scalability. The research also enhances understanding of the hydrogen evolution reaction, leading to the development of improved catalyst materials, optimized electrode structures, and enhanced reaction conditions. These technological advancements have broader implications in electrochemistry and catalysis beyond hydrogen evolution, impacting various fields and applications.

1.5. Scope of the Study

The scope of this study was limited to synthesis of Cu/MoS_2nanostructure by using facile electrochemical deposition method, characterization of the Cu/MoS_2 nanostructure using SEM, TEM, HRTEM, EDS, and XRD techniques, and examination of the performance of Cu/$MoS_2$for HER.

CHAPTER TWO

2. Literature Review

2.1. Hydrogen Energy

The principal drivers behind a sustainable energy vision of our future centre on the need to reduce global carbon dioxide emissions and improve local (urban) air quality, ensure security of energy supply and move towards the use of sustainable local energy resources, and create a new industrial and technological energy base, crucial for future economic prosperity(Edwards et al., 2007). Despite the advances in renewable energy, fossil fuels seem to continue to dominate the energy sector in near future(Apak et al., 2017). Figure 1 shows hydrogen as an energy carrier linking multiple hydrogen production methods through storage to various end-users.

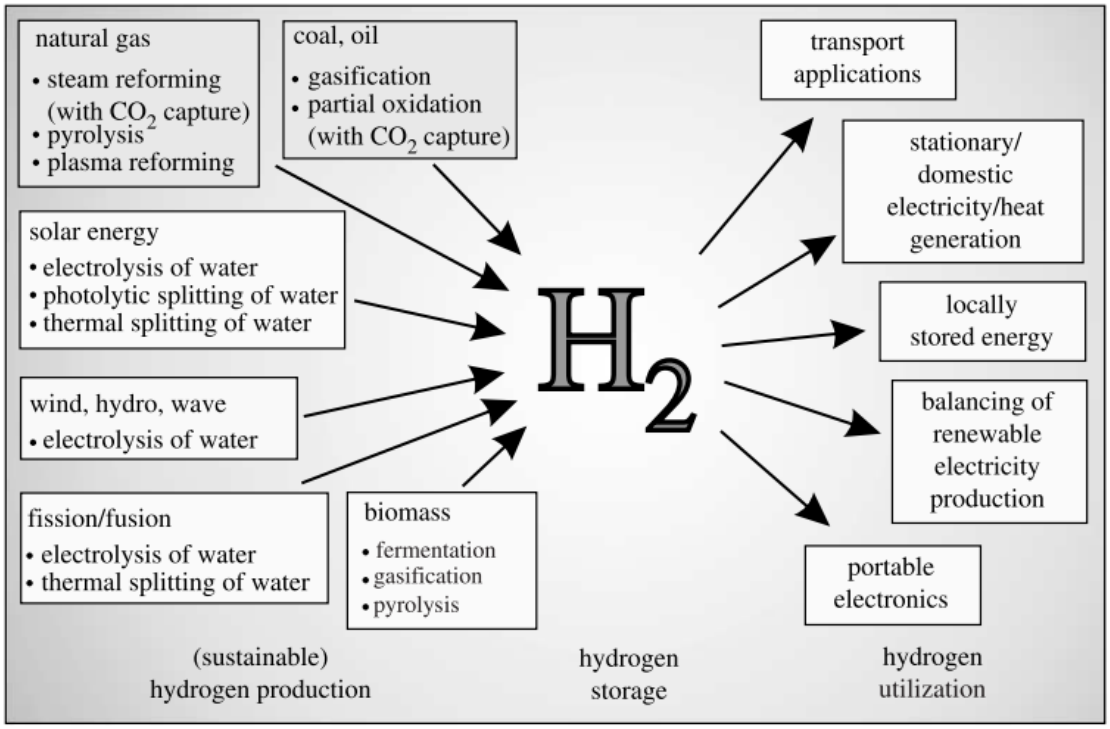

FIGURE1:Hydrogen as an energy carrier linking multiple hydrogen production methods, through storage to various end-users. Shaded production routes can involve substantial carbon dioxide (by-product) generation(Edwards et al., 2007).

All modern-day assessments of global energy futures take the view that the growth in demand must be met increasingly by a diverse energy mix, including renewable or sustainable energy sources(Edwards et al., 2007).Hydrogen energy is seen as a renewable power system that is an alternatively convenient storage and transmission vector(Apak et al., 2017).Hydrogen used as fuel, a storage medium for electricity, transportation and portable electronics(Rosen & Koohi-Fayegh, 2016).Free hydrogen does not exist abundantly and is mainly present in compounds like hydrocarbons and water (Tiwari et al., 2018). As summarized in Figure 1, hydrogen can be obtained from diverse resources, both renewable (hydro, wind, wave, solar, biomass and geothermal) and non-renewable (coal, natural gas and nuclear) (Edwards et al., 2007).

2.1.1Electrocatalytic Water Splitting

A possible solution to the problem of energy sustainability is electrochemical water splitting for large-scale hydrogen synthesis. An aqueous electrolyte, an anode, and a cathode make up the majority of electrolyzers. In order to accelerate the overall water splitting reaction, the bifunctional HER-OER catalysts are applied to both the anode and cathode respectively.This can take place at the anode and cathode when an external voltage is supplied between the two electrodes(Samantara & Ratha, 2019). Depending on the electrolytes in which water splitting proceeds, the water splitting reaction can be described as shown below(Briefs & Materials, n.d.).

Total reaction: $2H_2O \rightarrow 2H_2 + O_2$ (1)

In acidic solution

Anode: $2H_2O \rightarrow 4H+ + O_2 + 4e^-$ (2)

Cathode: $4H+ + 4e^- \rightarrow 2H_2$ (3)

In neutral or alkaline solution

Anode: $4OH^- \rightarrow 2H_2O + O_2 + 4e^-$ (4)

Cathode: $4H_2O + 4e^- \rightarrow 2H_2 + 4OH^-$ (5)

The bulk of known bifunctional HER-OER catalysts function in alkaline electrolytes. Compared to acidic electrolytes, alkaline electrolytes enable the substitution of expensive

transition metal and/or functional catalysts for expensive precious Pt, Ir, or Ru-based metal catalysts (Tiwari et al., 2018)

However, HER is slower in alkaline media than acidic media. This is because water dissociation half-cell reaction takes place at the cathode (HER) of electrolysers operating under alkaline conditions instead of anode (OER) for electrolysers operating under acidic conditions(Tiwari et al., 2018). The theoretical potential of the electrochemical water splitting is 1.23 V, but due to the sluggish reaction kinetics and poor activity of the working electrodes, the water splitting potential exceeds 1.8 V, in practice, which includes two half reactions of HER at the cathode and OER at the anode(Anantharaj et al., 2016). Higher potential values of cathodic potential (E_c)and anodic potential (E_a) vs the normal hydrogen electrode (NHE) than the theoretical value are needed to carry out the water splitting mainly for overcoming the cathodicoverpotential (η_c) and anodic overpotential (η_a) , others overpotential (η_{other}) and reactions' activation hindrances including contact resistance and solution resistance. Therefore, the potential of the overall water splitting is given as follows (Anantharaj et al., 2016):

$$V_{op} = 1.23V + \eta + |\eta_c| + \eta_{other} \quad (6)$$

In view of this, the primary challenge for research is to develop efficient bifunctional water splitting electrocatalysts, preferably based on low-cost and earth-abundant elements so that η_a and $|\eta_c|$ are minimized and the water splitting efficiency is improved

2.1.2 Mechanism of Hydrogen Evolution Reaction

HER with two-electron transfer is generally recognized as an adsorption–desorption process of the intermediates possibly involving three principal steps for the reduction of protons in acidic media or water molecules in alkaline media to produce H_2(Huang et al., 2020).

(i) In acid medium:

1: Volmer reaction: In this step the H^+ ion combine with an electron and get adsorbed onto the catalytic active site (Briefs & Materials, 2018).

$$H^+(aq) + e^- \rightarrow H_{ads} \quad (7)$$

2: Heyrovsky reaction: The adsorbed hydrogen atom interacts with a proton from the solution and an electron producing an electrochemical desorption (Alonso-Vante et al., 2019).

$$^{*}H_{ad} + e^{-} + H^{+} \rightarrow H_2 + * \quad (8)$$

3 Tafel reaction: Another possible way for desorption of hydrogen is the recombination reaction or Tafel reaction in which two adsorbed hydrogen atoms form molecular hydrogen as (Tiwari et al., 2018) .

$$H_{ads} + H_{ads} \rightarrow H_2(g) \quad (9)$$

(ii) In alkaline medium:

Since in the alkaline medium the OH^{-} ions are abundantly present, so the reaction proceeds as per the following steps:

1. Volmer reaction: proceeds as indicated in eq. (4). The molecular water is reduced by an electron to generate an adsorbed hydrogen atom at the electrode surface(Alonso-Vante et al., 2019):

$$M + H_2O + e^{-} \rightarrow M\text{-}H_{ad} + OH^{-} \quad (10)$$

2 . Heyrovsky reaction: The adsorbed hydrogen atom couples with a water molecule and an electron allowing the electrochemical desorption of hydrogen (Briefs & Materials, 2018).

$$M\text{-}H_{ad} + e^{-} + H_2O \rightarrow H_2{}^{+}* + OH^{-} \quad (11)$$

3 . Tafel reaction: Chemical desorption (Huang et al., 2020)

$$2M\text{–}H_{ads} \rightarrow 2M + H_2 \text{ (both acidic and alkaline mediums)} \quad (12)$$

Both Volmer–Heyrovsky and Volmer–Tafel pathways involve the formation of an H intermediate (H*). The rate-determining step in the HER process is defined as the reaction step with the largest kinetic activity barrier, and it is very important to determine the rate-determining step(Zhao et al., 2021).It has been revealed that for a Tafel RDS (Rate Detarmaning Step) the slope is 29 mV/dec, whereas for the Heyrovsky and VolmerRDS, the slopes are 39 and 118 mV/dec. respectively (Briefs & Materials, n.d.) . If the Volmer reaction is the rate-determining step, then the catalytic material needs more edges and cavities in the surface to promote hydrogen adsorption and electron transfer. However, if the Heyrovsky or Tafel reaction is the rate-limiting step, then increasing the reaction area can

increase the reaction rate(Zhao et al., 2021). ΔG_{H^*} is an important criterion to estimate the activities of HER catalysts (Huang et al., 2020). Generally the material activity with respect to the value of ΔG_H is represented in form of Volcano plot (Figure. 2) (Briefs & Materials, n.d.). According to the Volcano plot when the value is close to zero, it shows that the catalyst has the best electrocatalytic performance in theory (Zhao et al., 2021).The strong interaction of H^* on the electrode surface ($\Delta G_{H^*}>0$) slow down the Volmer step leading to a limited turnover rate. On the other hand, the weak interaction ($\Delta G_{H^*}<0$) speed up the Volmer step and hampers the Tafel or Heyrovsky reaction steps (Briefs & Materials, n.d.).

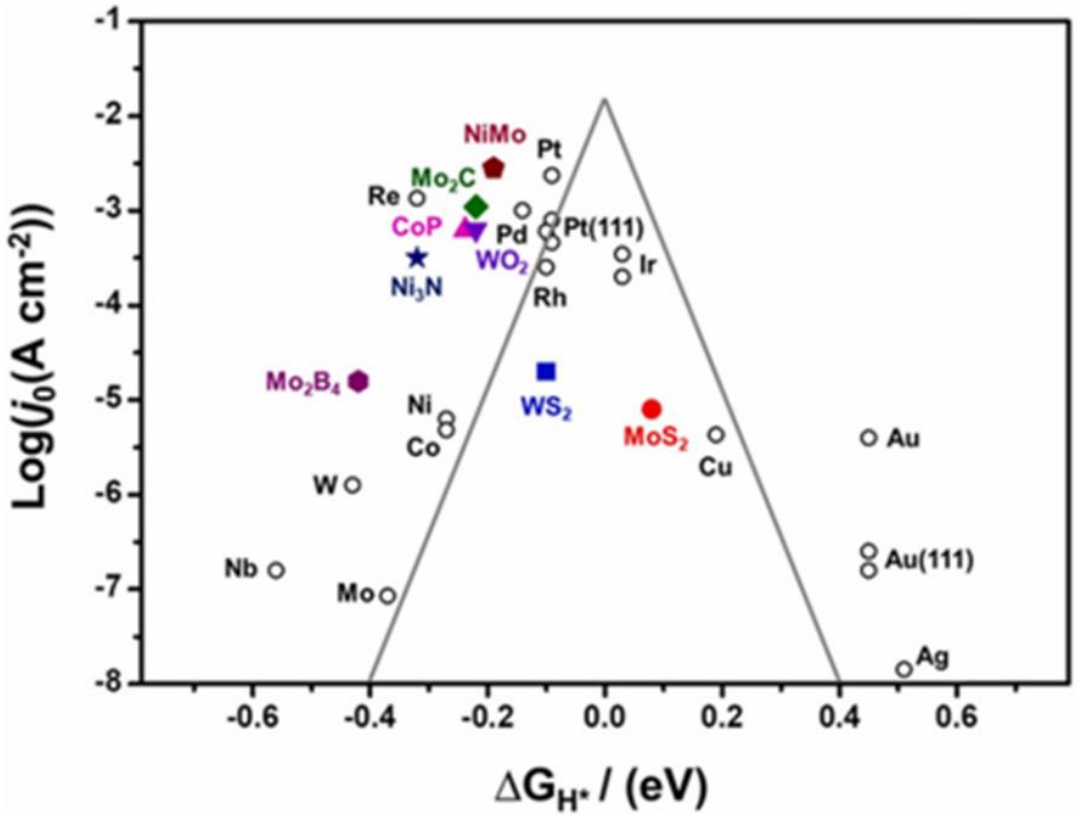

FIGURE2: Volcano plot of experimentally measured exchange current density as a function of the DFT-calculated Gibbs free energy of adsorbed atomic hydrogen (Briefs & Materials, n.d.).

The Sabatier principle, that states that in heterogeneous catalysis and electrocatalysis the optimal activity can be achieved on a catalytic surface having intermediate bonding energies with reactive intermediates (Alonso-Vante et al., 2019). Platinum and Pt-group metals (PGM) remain the most active HER electrocatalyst due to their ΔG_{H^*} close to zero and high exchange current density, j_0 .It is important to mention that ΔG_{H^*} is an intrinsic property of electrocatalysts. However, it should be distinguished that in practice the activity of a HER

electrocatalyst is collectively influenced by many other factors as well including but not limited to: the conductivity, the crystallinity, the roughness and the interactions with supporting materials (Briefs & Materials, n.d.). From molybdenum based nanomaterials, MoS_2 nanosheets have received widespread attention in the field of electrocatalysis because of their S-edges with optimal hydrogen adsorption Gibbs free energy (ΔG_{H^*} = 0.06 eV), which is close to 0 eV(Sun & Meng, 2021). The computational free energy of atomic hydrogen bonding to the MoS_2 edge was close to that of Pt (Figure 3) raising the possibility of MoS_2 as a promising HER electrocatalyst in theory.

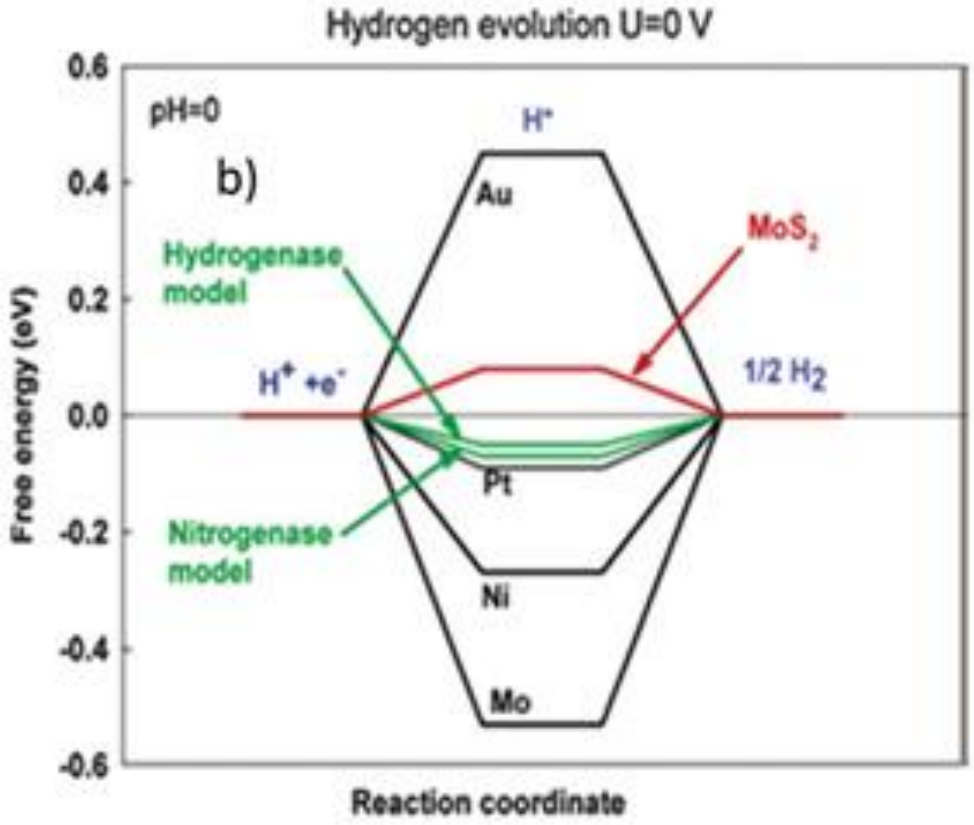

FIGURE3: Calculated free energy diagram for hydrogen evolution relative to the standard hydrogen electrode at pH 0.4 (Zou & Zhang, 2015a).

2.2Measurements Criteria for Catalytic Activity

2.2.1Overpotential

The thermodynamic equilibrium potentials in any electrolytes for the water splitting are 0 and 1.23 V (both versus RHE: reversible hydrogen electrode) for catalyzing HER and OER, respectively. However, because of those inherent kinetic obstacles, a practical process requires an additional potential, typically known as the overpotential and represented by the symbol η ((Anantharaj et al., 2016). Three different types of overpotentials namely: the activation overpotential, concentration overpotential, and resistance overpotential, are present throughout the water splitting process. An appropriate electrode material can significantly lower the activation overpotential, an inherent feature of the electrocatalysts (J. Wang et al., 2020). The overpotential is often determined from the polarization curve produced by charting the current density vs the overpotential for a particular current density. The greater performance of the electrocatalyst is shown by the lower value of the overpotential at the same current density (Bhat & Nagaraja, 2021).

2.2.2Tafel Slope and Exchange Current Density

Tafel slope provides the insights into the reaction mechanism of a catalysis process (HER or OER) on the electrocatalyst surface. It is generally calculated to study the intrinsic properties of a particular electrocatalyst. The Tafel plot shows the relation between the iR-corrected overpotential and current density as per the following equation(Briefs & Materials, n.d.).

$\eta = a + b \log j$……………………………………………………………(16)

Here η, a, b and j are the overpotential, Tafel constant, Tafel slope and current density respectively.

The Tafel plot can be derived from the polarization curves by plotting log of current density (log j) against overpotential (η).The Tafel slope can be used to deduce the possible kinetic rate of the electrocatalyst and determine the reaction mechanism.The smaller value of Tafel slope represents that increasing the same current density needs the smaller overpotential, which suggests a faster charge transfer kinetic(J. Wang et al., 2020).The HER proceeds via two steps as Volmer step (adsorption of active hydrogen) followed by either Tafel or Heyrovsky steps (for desorption in form of molecular hydrogen). It has been stated that the theoretical Tafel slopes of 118, 39 and 29 mV/dec. are assigned to the Volmer, Heyrovsky

and Tafel reaction pathways(Briefs & Materials, n.d.). The rate-determining step in the HER process is defined as the reaction step with the largest kinetic activity barrier, and it is very important to determine the rate-determining step. Ifthe Volmer reaction is the rate-determining step, then the catalytic material needs more edges and cavities in the surface to promote hydrogen adsorption and electron transfer. However, if the Heyrovsky or Tafel reaction is the rate-limiting step, then increasing the reaction area can increase the reaction rate (Zhao et al., 2021).Exchange current density (j0), which reflects the intrinsic rate of the electron transfer between an analyte in solution and the electrode under equilibrium conditions and is only correlated to the catalyst materials, electrolyte, and temperature is the corresponding value of j calculated from the Tafel equation when the value of η is equal to zero. In other words, the more exchange current density there is, the more active the water-splitting catalyst will be Briefly,effective electrocatalyst for water electrolysis typically has a low overpotential, a small Tafel slope, and a high exchange current density(Zou & Zhang, 2015a)

2.2.3Electrochemical Active Surface Area (ECSA)

Electrochemical active surface area (ECSA) is also used to evaluate the total number of active sites on a given surface for a certain electrocatalysts (J. Wang et al., 2020) . As the area is more exposed, so are the active sites enhancing higher mass transfers, facilitating the rate of reaction. It will allow us to determine quantitatively the reacting interface of a given catalyst. The most common method of calculating ECSA is based on the electric double layer capacitance (C_{dl})(Gicha et al., 2021). ECSA can be determined as,

$$ECSA = C_{dl} / C_s \quad \text{.....(17)}$$

Where C_{dl} is double layer capacitance and C_s is specific capacitance.

Instead the double layer capacitance (C_{dl}) can be obtained from the cyclic voltammograms of the respected materials. It can be derived either from the static cyclic voltammograms recorded at different sweep rates in a non-Faradic potential region ,Cs is the specific capacitance of an atomically smooth flat catalytic surface and the value assumed to be in a range of 20–60 μF/cm^2.Further the roughness factor (Rf; active site per unit surface area) can be obtained from the ECSA by simply dividing the geometrical surface area of the electrode as per the following equation(Briefs & Materials, n.d.),

$R_f = ECSA / S_{geo}$……(18)

2.2.4 Stability

Stability, as another crucial important parameter, is utilized to assess the ability of a catalyst to maintain activity with a long-term operation period(J. Wang et al., 2020).There are two methods for characterizing the electrocatalytic stability of a HER catalyst. One method is to measure the current variation with time (i.e., the I–t curve). For this measurement, it would be better to set a current density larger than 10 mA cm^2 for a long period of time (>10h). The other method is to conduct the recycling experiment by performing CV or LSV. The number of cycles should be larger than 5000 times to elucidate the stability of a material(Zou & Zhang, 2015b)

2.3. Structure of MoS_2

MoS_2 is composed of stacked planes of Mo atomic layers and S layers. The Mo−S bonds are controlled by strong covalent bonds and adjacent layers are held together by van der Waals interactions. MoS_2 has three different crystal-phase structures: 1T, 2H, and 3R where digits represent the S−Mo−S layer number in the unit cell and the letters stand for hexagonal, rhombohedral, and tetragonal, respectively. Among them, 2H is the most stable structure, and 3R is easy to change into 2H under heating (Sun & Meng, 2021)**.** The metastable 1T phase is not found in nature but can be made via intercalation of the 2H-MoS_2 lattice with lithium or organolithium compounds. In the 1T phase the Mo atom is Octahedrally coordinated to six neighboring S atoms whereas in 2H phase, each Mo center is prismatically coordinated by six surrounding S atoms as seen in (Figure 4) (Tang & Jiang, 2016).

Among 1T, 2H, and 3R, 2H is the most stable structure and 3R is easy to change into 2H under heating but due to the different fillings in d_{xy}, d_{xz}, d_{yz}, $d_{x^2-y^2}$, and d_{z^2} orbitals of Mo as shown in (Figure 5), MoS_2 shows different electronic structures and electronic properties. Complete filling of the 2H phase of d orbitals has semiconducting behavior materials and the partial filling 1T phase has metallic behavior. As a result, the electronic structure of MoS_2 can be successfully altered by modifying the different filling degrees of the d orbital that affects the efficiency of electrocatalysis(Sun & Meng, 2021).

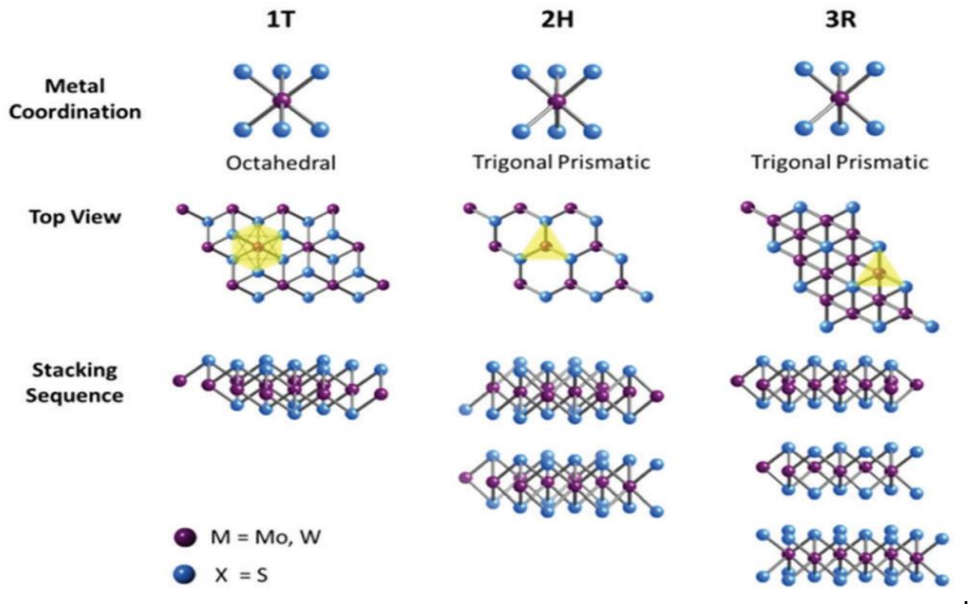

FIGURE4**:**Metal-coordinations and stacking sequences of TMD structural unit cells. Metal coordination can be either octahedral or trigonal prismatic. The octahedral coordination allows stacking sequences, which yield a tetragonal symmetry (1T). Dissimilar stacking sequences of trigonal prismatic single layers can give rise to different symmetries: hexagonal symmetry (2H) and rhombohedral symmetry (3R)(Toh et al., 2017).

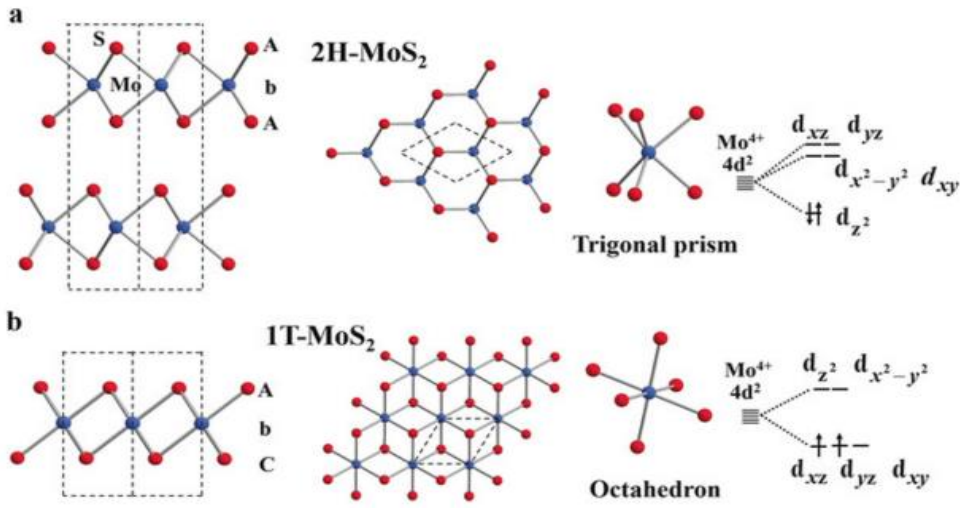

FIGURE5**:**(a) Crystal structure of 2H-MoS_2 and the ligand splitting for 4d orbitals of Mo atoms with trigonal−prismatic coordination. (b) Crystal structure of 1T-MoS_2 and the ligand splitting for 4d orbitals of Mo atoms with octahedral coordination(Yin et al., 2022).

2.4. MoS_2Based Nanomaterial's for Hydrogen Evolution Reaction

The study of MoS_2 on electrochemical HER can be traced to the 1970s which showed that bulk MoS_2 crystals were non-reactive toward HER. As a result, MoS_2 has not been considered as a promising hydrogen evolution electrocatalyst for a long time (Zou & Zhang, 2015b). MoS_2nanosheets have received widespread attention in the field of electrocatalysis because of their S-edges with optimal hydrogen adsorption Gibbs free energy (ΔG_{H^*} = 0.06 eV) which is close to 0 eV(Sun & Meng, 2021) . However, it has been demonstrated that the negative hydrogen binding energy (ΔG_{H^*}) for MoS_2 is quite low indicating the strong adsorption of H on the MoS_2surfacefavoring the reduction of H^+ while it hinders the desorption of H_2. Certain current studies report that heteroatom doping into MoS_2 can regulate the electron density around the Fermi level of MoS_2 and thus increasing the activity sites towards better HER performance (Liu et al., 2020). On the other hand, it was reported that the Mo-nitrides such as MoN and Mo_2N catalyst showed highly efficiently HER catalytic performance owing to the high-valence, similar electronic structures to platinum-group metals, and high conductivity features (Liu et al., 2020). Interestingly, due to a low temperature synthesis process, a large amount of chlorine remained inside the MoS_2 structures, which played an important role in the phase formation of MoS_2. Due to the presence of Cl, the 1T phase of MoS_2 together with the 2H phase was observed, which improves the conductivity of MoS_2 and thus increased the HER performance (Anh Ho et al., 2021). In steam-etched MoS_2 flake, the free energy barrier of the discharge step is reduced to be comparable with that of the following desorption or combination step resulting in a significant drop of the slope to 96 mV/dec. The improved Tafel slope originates from the generated MoS_2-edges on MoS_2 basal plane which effectively decreased the activation energy (Z. Wang et al., 2018). The V-doped MoS_2 showed better catalytic performance than pure MoS_2 due to their better in-plane conductivity, higher carrier concentration, and shorter electron transfer path (Sun & Meng, 2021). The band gap observably decreased after V doping indicating that the electronic structure of MoS_2 was changed. Moreover, V doping in the MoS_2 lattice could cause the interaction between the incorporated V atoms and neighbor Mo atoms and thus activating the valence electrons resulting in improved electrical conductivity of MoS_2(Sun & Meng, 2021). Also, Bao et al. reported on Co-doped MoS_2. In their work, Co-doping could increase the electron density on the S atom, gain the optimal ΔGH^*, and reduce the energy level of MoS_2 in-plane to enhance HER activity. Notably, the

doping amount of Co may lead to excessive reduction of electrons on the S atom and the interaction between the H atom and S atom became stronger resulting in the poor surface stability of MoS_2 which was also not conducive to HER activity (Yin et al., 2022). Besides, the role of doped Ni in triggering the HER performance of MoS_2 was identified by Chen's group (Sun & Meng, 2021) . In their work, Ni-doped MoS_2 exhibited strong interaction between Ni−S bonds and regulated the local electronic structures. The change of electronic structure affected ΔG_{H^*} and improved the catalytic kinetics. According to a volcano plot of the exchange current density as a function of the DFT calculated Gibbs free energy of adsorbed atomic hydrogen, the value of Cu just lies below those of the noble Pt-group metals. The combination of Cu with MoS_2 appears to be a promising way to increase the conductivity and improve the HER performance(J. Cao et al., 2017b). The combination of Cu with MoS_2 appears to be a promising way to increase the conductivity and improve the HER performance, this is because the Cu NPs can act as electron donors, providing electrons to the MoS_2 nanoparticles, which can act as electron acceptors. This transfer of electrons canpromote the catalytic activity of both materials, leading to a greater overall catalytic activity than either material alone as shown in (Figure 6) ,the obtained hybrid contains a large number of active HER catalytic sites due to the abundance of accessible edges resulting from the small size and irregular shape of MoS_2.

The use of Cu NPs not only improved the electrical conductivity of the catalyst but also further enhanced the catalytic activity by a synergistic effect with nano-sized MoS_2(J. Cao et al., 2017b). Gudalet al reported that the presence of Cu in MoS_2 significantly boosts the HER catalytic efficiency. Cu@MoS_2 exhibits outstanding electrocatalytic performance toward the HER with a small overpotential of 131 mV for an areal current density of 10 mA/cm^2 , a Tafel slope of 51 mV/dec, and long term stability. In the as-prepared Cu@MoS_2, the porous structure and 1T MoS_2 can simultaneously activate the basal plane and supply more active edge sites and the doping of Cu atoms lead to electron transfer between Cu and MoS_2 (Wu et al., 2019). However, Feng Li et al reported that the Cu doped MoS_2/rGO hybrid catalyst exhibits excellent HER activity with a small Tafel slope value and large cathodic current. In the study, the composite of Cu and MoS_2 on the reduced graphene oxide (rGO) i.e. (Cu-doped MoS_2/rGO) showed high catalytic activity toward hydrogen evolution reaction (HER). It was found that the presence of rGO improved the electrical conductivity of the

catalyst, and the MoS_2nanoflowers (NFs) with a higher number of exposed edges exhibited higher HER activity (F. Li, Zhang, et al., 2015).

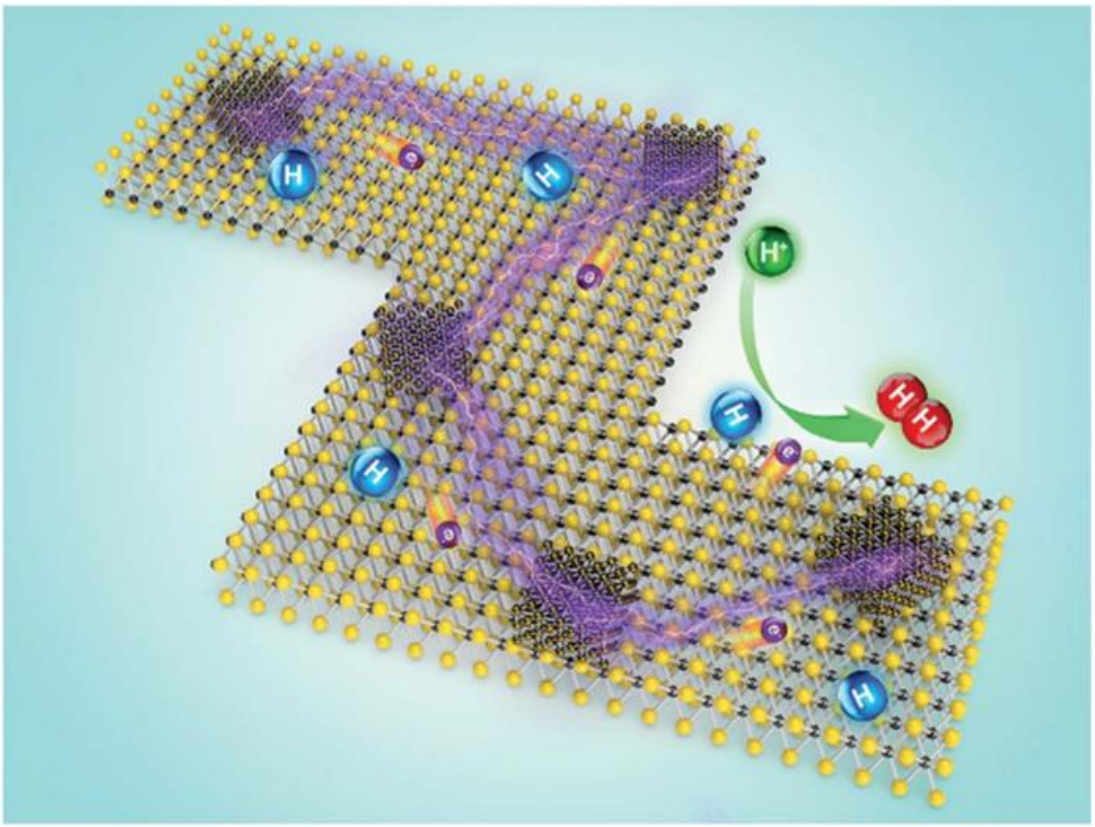

FIGURE6:Schematic illustration of the mechanism governing the electrocatalytic HER on the Cu/MoS_2

The addition of Cu particles not only enhanced the electrical conductivity of the catalyst but also further improved the catalytic activity by synergistic effect with MoS_2 catalyst (i.e., MoS_2/Cu) synthesized by frugal and facile approach,MoS_2/Cu electrocatalyst demonstrated good Tofel slope (~75.8 mV dec^{-1}), and excellent electrocatalytic activity and high stability in the alkaline solution (Ilyas, Raziq, Ali, Zada, Ilyas, Shaha, & Wang, 2021).

2.5. Typical Synthetic and Fabrication Methods of MoS_2Nanomaterials

Many synthesis methods of the MoS_2-based NSs have been reported including mainly solvothermal (hydrothermal) and electrochemical deposition methods. In order to further understand the influence of the synthesis methods on the structure and composition of MoS_2-based NSs , we introduce some common synthesis methods as follows.

2.5.1 Hydro (solvo) thermal Method

Hydrothermal method refers to purely heterogeneous reactions using water as media in a sealed steel pressure container with Teflon liners. It is capable of synthesizing advanced inorganic materials in high yield. Typically, the temperature of the hydrothermal process is in the range of 100–200 °C and the pressure is generated autogenously (F. Wang et al., 2015). The benefit of fast reaction kinetics and quick processing time combined with the mild temperatures make it a potential method for efficiently and inexpensively preparing homogeneous goods on a wide scale (X. L. Li et al., 2020). Hongwei Cao *et al* fabricated a defect-rich mixed 1T-2H MoS_2nanoflowers through a hydrothermal process (H. Cao et al., 2020). In this typical procedure, $NH_4Mo_7O_{24}{\cdot}4H_2O$ and CH_4N_2S were dissolved in a round bottom flask with 20 ml deionized water, 40ml ethanol and 20ml glycerin. Then 0.97 ml hydrochloric acid was added to regulate the pH of the mixed solution to ~0.95. After ultrasonic treatment for 15 minutes, the mixed homogenous solution was transferred into a Teflon stainless steel autoclave (100 ml) and heated to 200 ℃ for 12h. After cooling to room temperature, the product was washed by deionized water and absolute ethanol for three times via centrifugation, respectively. Then the sample of MoS_2 was obtained after being dried at 80 ℃ for 12 h, and denoted as MoS_2-water-ethanol-gly. For preparing MoS_2-water, 80 ml deionized water was introduced without any ethanol or glycerin for a hydrothermal process. Similarly, MoS_2-water-ethanol was acquired in the solvothermal condition with 20 ml deionized water and 60 ml ethanol, while MoS_2-water-gly was prepared using 60 ml DI water and 20 ml glycerin.Yuxia Jiang*et al*, using ammonium molybdate as molybdenum source and thiourea as sulfur source, MoS_2 hollow microspheres with a diameter of about 2 μm are successfully synthesized by adding ionic liquids ([EMIM] Cl). When ([EMIM] Cl) is replaced with ([EMIM] Br), new structure of hollow core/shell as well as double shell MoS_2 microspheres are hydrothermally synthesized (X. L. Li et al., 2020). H. Akram*et al* MoS_2nanomaterials prepared using one-pot solvothermal method (Akram et al., 2014). In a typical procedure of ammonium molybdate $(NH_4)_6Mo_7O_{24}$, $4H_2O$), elemental sulfur, lithium hydroxide monohydrate ($LiOH{\cdot}H_2O$), of ammonium carbonate $(NH_4)_2CO_3$ and 8 ml hydrazine monohydrate ($N_2H_4{\cdot}H_2O$) were put in a teflon lined stainless steel autoclave. Finally the whole mixture was solvothermaly treated in a Teflon-lined stainless steel autoclave for 24 h under 180◦.The final product was washed thoroughly with deionized water and dried at 60 °C overnight before further use. Also Shige Wang *et al* synthesized

MoS_2 or MoS_2-PEG nanosheets with desirable sizes using a hydro-thermal or solvo-thermal approach. For the synthesis of MoS_2nanosheets with the diameter of 50 nm (denoted as MD50), $(NH_4)_2MoS_4$ was dissolved into 60 mL distilled water by vigorously magnetic stirring to get a homogenous solution. The solution was then transferred into a 100 mL polyphenylene-lined stainless steel autoclave and maintained at 220 C for 12 h. The hydro(solvo)thermal method has been widely used in the preparation of two-component or multi-component TMD-based composites, such as MoS_2/CdS, MoS_2 /TiO_2, MoS_2–graphene (G), Zn x Cd $_{1-x}$ S/MoS_2 , MoS_2 /$ZnIn_2S_4$, Mo_2 G/CdS, ZnS/G/MoS_2 , TiO_2/G/ MoS_2 , and In_2S_3 /MoS_2 /CdS. However, the disadvantages of this method are also obvious. For example, it is difficult to realize precise control of the layer numbers of TMDs (Lu et al., 2016).

2.5.2. Chemical Vapor Deposition (CVD) Method

CVD synthesis process adopts a bottom-up approach, to control morphology, crystallinity and defects. This method extends control of different process parameters so as to obtain high quality, high purity 2-D nanomaterial with controlled properties (Krishnan et al., 2019). This method facilitates development of novel types of 2-D nanosheets and their hybrids, by combining variety of precursors in different forms. CVD indicates development of thin films in large scale by chemical reaction of vapors over substrate. Figure 5 shows the schematic diagram of this method (Gupta et al., 2020). Basic CVD method is a direct evaporation also called vapor solid growth method. It yields small flakes of less quantity but of high quality as a single layer on a substrate. However, it suffered from discontinuous 2D-MoS_2 films, contributing to development of vapor phase growth. In this, thin molybdenum layer of required length is formed on substrate and sulfur vapor is made to flow over it. Numerous vapor chemical deposition methods have been developed for wafer scale growth, which resulted in large sided triangular morphologies of 2D MoS_2(Krishnan et al., 2019). CVD method utilizes one of the three different types of precursors. First one being ammonium thiomolybdate solution[$(NH_4)_2MoS_4$], second is molybdenum trioxide powder[MoO_3] , and third is elemental molybdenum(Krishnan et al., 2019) . When using first type of precursor the compound is made to decompose during various annealing stages to produce MoS_2 film. Crystal grain sizes are dependent on type of substrates utilized for growth of MoS_2 film. Larger crystal sizes are formed while using sapphire substrate than by SiO_2. FETs with n-type behavior are fabricated by using MoS_2. They had a field–effect mobility of 6 cm^2 /Vs

along with an on/off ratio of about ~10^5. It was reported that when graphene on Cu foil was used as substrate in an environment of argon gas, the resultant was a 2-5 nm grain size (Sun et al., 2017). Additionally, MoS_2 nucleating as wrinkles on surface of graphene lead to formation of hexagonal MoS_2. When $(NH4)_2MoS_4$ was dip-coated on an insulating substrate, it produces transferrable, high crystalline three-layer MoS_2 (Sun et al., 2017). Balendhran et al. developed a bulk synthesis methodology in which two step processes is used when second type of precursor (MoO_3) is used. MoO_3 is first evaporated on an arbitrary substrate, followed by sulfidation process in a quartz tube. This two-step method is more preferred because of higher electron mobility. FET of n-type, produced by this method exhibited an on/off ratio of ~10^4 along with field–effect mobility of 0.02 cm^2 /Vs. Various combinations of temperatures and steps were experimented and reported to customize electronic property as per need of FET devices and applications. It was reported that when process was conducted using powdered MoS_2 instead of MoO_3, it yielded MoS_2 flakes having triangular shape with high crystallinity(Krishnan et al., 2019). Further $MoCl_5$ and elemental sulfur were used as precursors to produce uniform and high quality mono and bilayer MoS_2 film of grain size ranging from micro to few nanometers. While using third type of precursor, a thin layer of molybdenum film is made to absorb into SiO_2 substrate and sulfurized at high temperature in inert atmosphere. Film formed by this precursor was a function of area covered by molybdenum absorbed over substrate, process temperature and type of substrate. Resultant reported by this were both n-type and p-type behavior films of MoS_2 with higher mobility ratios ranging from .004 cm^2 /Vs to .04 cm^2 /Vs with grain sizes of 5 nm to 30 nm. This process effectively grows MoS_2 atomic layers by coalescence of triangularly shaped single crystals, which results in large scale and few-layered MoS_2 displaying a high level of crystallinity. Few limitations reported in this method are lack of pattern-ability due to random nucleation of precursor and scalability. Primary reason is attributed to competition between lateral growth, which increases size of product and vertical growth, resulting in increased layers, especially under prolonged reaction. It was also reported that by using CVD process (by using second precursor) aligned edge – terminated vertically stacked MoS_2 sheets were also formed, which finds a prominent place as biosensor and catalyst, due to exposed active of MoS_2 sheets (Gupta et al., 2020). Similarly, nanosheets can easily be doped and functionalized by introducing one additional precursor source in mixture. In contrast, tailoring atomic level properties, controlling

stoichiometry and defects in 2-D materials will require further optimizations, and remains significant challenge in growth of CVD (Sun et al., 2017).

2.5.3 Electrochemical Deposition Method

Molybdenum disulfide (MoS_2)-based nanomaterials have been widely studied for their potential applications in various fields such as energy storage, catalysis, and electronics. Among the various methods used for synthesizing MoS_2-based nanomaterials, electrodeposition has emerged as a promising technique due to its simplicity, cost-effectiveness, and ability to precisely control the size and morphology of the resulting materials. Several studies have reported the synthesis and characterization of MoS_2-based nanomaterials using electrodeposition for water splitting applications. For instance, Liuqing Pang et al. (2019) reported the synthesis of MoS_2-based nanomaterials on a conductive carbon fiber substrate using a simple and efficient one-step electrodeposition method. The authors found that the resulting MoS_2-based nanomaterials exhibited excellent catalytic activity for hydrogen evolution reaction (HER) and oxygen evolution reaction (OER) in alkaline media, attributed to the high surface area and the presence of active sites on the MoS_2 nanoparticles (Pang et al., 2019) .

Similarly, Rastogi et al. (2021) synthesized MoS_2-based nanomaterials on a conductive substrate using a two-step electrodeposition method and demonstrated their potential as bifunctional electrocatalysts for HER. The authors found that the resulting MoS_2-based nanomaterials exhibited excellent catalytic activity and stability for both HER, attributed to the high surface area and the presence of active sites on the MoS_2 nanoparticles (Rastogi et al., 2017). In another study, Rastogi et al. (2017) synthesized MoS_2-based nanomaterials on a conductive substrate using a facile electrodeposition method and demonstrated their potential as a highly efficient electrocatalyst for HER in acidic media. The authors found that the resulting MoS_2-based nanomaterials exhibited excellent catalytic activity and stability for HER, attributed to the high surface area and the presence of active sites on the MoS_2 nanoparticles (Rastogi et al., 2017). However, Ying Zhang et al. (2021), synthesized MoS_2-based nanomaterials on a conductive substrate using a facile electrodeposition method and demonstrated their potential as a highly efficient electrocatalyst for HER in basic media. The authors found that the resulting MoS_2-based nanomaterials exhibited excellent catalytic

activity and stability for OER, attributed to the high surface area and the presence of active sites on the MoS_2 nanoparticles (Y. Zhang et al., 2021).

Additionally, several studies have reported the synthesis and characterization of MoS_2-based nanomaterials using electrodeposition for energy storage applications. For instance, Li et al. (2020) reported the synthesis of MoS_2-based nanomaterials on a nickel foam substrate using electrodeposition and demonstrated their potential as an anode material for lithium-ion batteries. The authors found that the MoS_2-based nanomaterials exhibited a high specific capacity and good cycling stability, attributed to the high surface area and the presence of active sites on the MoS_2 nanoparticles. Similarly, Zhang et al. (2021) synthesized MoS_2-based nanomaterials on a conductive substrate using a two-step electrodeposition method and demonstrated their potential as an anode material for lithium-ion batteries. The authors found that the resulting MoS_2-based nanomaterials exhibited a high specific capacity and excellent cycling stability, attributed to the high surface area and the presence of active sites on the MoS_2 nanoparticles. In another study, Yang et al. (2021) synthesized MoS_2-based nanomaterials on a nickel foam substrate using electrodeposition and demonstrated their potential as an anode material for sodium-ion batteries. The authors found that the resulting MoS_2-based nanomaterials exhibited a high specific capacity and excellent cycling stability, attributed to the high surface area and the presence of active sites on the MoS_2 nanoparticles. The electrodeposition method has several advantages for synthesizing MoS_2-based nanomaterials for energy storage applications. One of the main advantages is that it enables direct deposition of MoS_2 on a conductive substrate, which can be easily scaled up for large-scale production. Additionally, the electrodeposition process can be controlled by adjusting the deposition parameters, which enables the precise control of the size, shape, and morphology of the resulting nanomaterials. Moreover, the method can be used to deposit MoS_2 in different forms such as nanosheets, nanorods, and nanoparticles.

In conclusion, electrochemical deposition method is a controllable, simple, eco-friendly and low cost approach to prepare catalysts for water splitting, which can fabricate some unique structure catalysts. Simultaneously, electrochemical deposition has also been proved to be a general and efficient synthetic means to synthesize monatomic catalysts (Wan et al., 2021). However, electrochemical deposition still has some disadvantages. The deposition efficiency is always affected by the electrode polarization and solvent effect derived from the charge transfer and concentration gradient in the solution. By considering all the aspects

mentioned above we have choice to synthesized Cu/MoS_2 on NF by a facile electrochemical deposition method for efficient HER

CHAPTER THREE

3. Material and Method

3.1. Study Site Description

Synthesis of Cu/MoS_2 NSs was conducted at the electroanalytical laboratory of Adama Science and Technology University, Department of Applied Chemistry. XRD characterization of the synthesized NSs was conducted at Adama Science and Technology University, Department of Material Science and Engineering and SEM, TEMand EDS characterizations were done at Chungnam National University, South Korea. The electrochemical water splitting experiment was conducted at the electroanalytical laboratory of Adama Science and Technology University, Department of Applied Chemistry

3.2. Chemicals and Reagents

NF (purity > 99.99%; surface density 346 g/cm^2 ; and thickness 1.6 mm) and FTO (resistivity 4.01x10-5 Ω.cm) obtained from MTI Korea ,HCl (37%) ,Ammonium molbdatethiosulphate. ($(NH_4)_2MoS_4$)(99.99%),KCl (99.95%), $Cu(SO_3)_2.5H_2O$ (97%), Ethanol (99.9%), KOH ACS reagent ≥85% pellets ,all chemicals were purchased from Sigma-Aldrich; and distilled water obtained from Adama Science and Technology University at Department of Applied Chemistry; were used in this work. All chemicals were used without any further purification.

3.3. Synthesis of MoS_2 and Cu/MoS_2Nanostructure Electrocatalysts

The MoS_2 NPs was synthesized by a two-step electrochemical deposition method. The Synthesis of MoS_2 NSs on nickel foam (NF) was carried out according to the recently reported literature with a slight modification by varying different deposition time(Quy et al., 2018). Prior to the deposition, the NF (20 mm length x 10 mm width x 1.6 mm thickness) was sonicated with 1 M HCl for 30 min to remove the oxide layer. Then, the HCl soaked NF was air dried to remove the moisture. The electrochemical deposition was performed in a three-electrode cell using the NF (size 1 cm x 1 cm) as the working electrode, platinum wire as the counter electrode, and Ag/AgCl electrode as the reference electrode. In the first step process, a voltage of -1.0 V was applied for four different

deposition time (100s, 200s, 300s, and 500s) in the electrolyte containing 7mM of ($(NH_4)_2MoS_4$) and 0.1M KCl . Then, the targeted MoS_2 NPs were rinsed by water and ethanol and air dried for 8 h. The deposition process Cu/MoS_2 NSs was based on a previously reported method with slight modifications by varying deposition time (Roy, Jadhav, Cho, &Seo, 2019). Frist 0.1M of $CuSO_4.5H_2O$ solutions were deposited on optimized (200s MoS_2) electrode for four different deposition time (60s, 80s, 100s and 120s) at a voltage of -1.0 V. After the deposition, the as-prepared Cu/MoS_2 NSswas rinsed with ethanol and water, followed by air drying for 8 h.

3.4. Characterization of Cu/MoS_2 Nanostructure

The crystal structure of the samples was analyzed by using X-ray diffraction (XRD) using XRD-7000 X-RAY DIFFRACTOMETER, SHIMADZU Corporation (Japan). The morphologies of the synthesized nanomaterial were characterized using scanning electron microscopy (SEM) and transmission electron microscopy (TEM) FE-SEM S-4700, Hitachi, and TEM, JEM-2100F, JEOL Ltd., Tokyo, Japan. The elemental composition and distribution were investigated with energy dispersive X-ray spectroscopy (EDS, JEOL-2010) coupled with scanning electron microscopy (SEM, S-4700), and electrochemical measurements were carried out by means of an Iviumstat electrochemical interface (Eindhoven, Netherlands).

3.5. Electrochemical Measurements

All electrochemical measurements were performed in a standard three-electrode system at Adama Science and Technology University, Applied Chemistry Department, using an Iviumstat (Eindhoven, Netherlands) workstation at room temperature while using the as-obtained catalysts on the NF as the working electrode (WE), Pt wire as the counter electrode (CE), and Ag/AgCl electrode as the reference electrode (RE) in 1M KOH as the electrolyte solution. For the HER, the Linear Sweep voltammetry (LSVs) measurements were carried out at the potential range from 0 to -1.5 V versus Ag/AgCl at a scan rate of 2 mV s^{-1}. Electrochemical impedance spectroscopy (EIS) was measured in a frequency range of 1×10^5 to 0.01 Hz at optimized potential of -1.16 V versus Ag/AgCl. Cyclic voltammetry (CVs) measurements were carried out from - 0.3 to - 0.2 V versus Ag/AgClat different scan rates of 20, 40, 60, 80, 100 and 120 mV s^{-1}, which were employed to estimate the double-layer capacitances (Cdl) of the catalysts. Chronoamperometry curves

were obtained with a constant current density of 10 mA cm^{-2}. The potentials measured were converted to a reversible hydrogen electrode (RHE) by using the following equation: (Gicha et al., 2021).

$$E_{RHE} = E_{Ag/AgCl} + 0.059 * pH + E_{Ag/AgCl}$$

The electrochemically active surface area (ECSA) was evaluated from the electrochemical double-layer capacitance (C_{dl}) by simple CV measurements in no apparent Faradaic region at different scan rates (Yu et al., 2017).

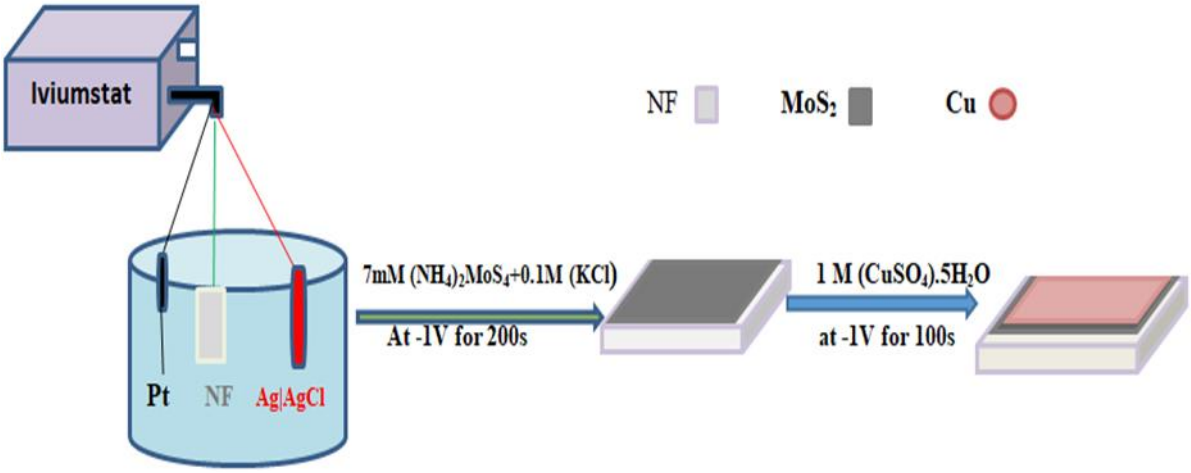

FIGURE7: Schematic illustration of the fabrication of Cu/MoS_2

CHAPTER FOUR

4. Result and Discussion

4.1. Fabrication and Characterization of Cu/MoS_2 Nanostructures

The Cu/MoS_2nanomaterials were prepared by a two-step electrochemical deposition method as illustrated in Figure 7. First, MoS_2 nanoparticles (NPs) were grown on the nickel foam (NF)through a simple and cost effective electrodeposition method at an applied potential of −1.0 V versus Ag/AgClat different deposition time of 100 s, 200 s, 300 s and 500 s Cu/MoS_2 NPs was cleaned with deionized (DI) water and left to dry and then, 0.1 M of $CuSO_4 \cdot 5H_2O$ solutions were deposited on optimized (200 s MoS_2) electrode for four different deposition time (60 s, 80 s, 100 s and 120 s) at a voltage of -1.0 V.The electrochemical deposition process leads to the change of silvery NF to black color when MoS_2 deposited,and then black colorchange toreddish brown when Cu deposited on MoS_2/NF, indicating successful deposition of the catalyst on the NF (AppendixFigure1).

4.1.1.XRD Analysis

The crystalline phases of the electrodeposited Cu/MoS_2 films were characterized by XRD, as (shown in Figure 8). Figure 8, reveals that there are no apparent XRD peaks of MoS_2, indicating that the MoS_2 films are amorphous(Quy et al., 2018). The peaks at 43.290, 50.40 and 74.130 with the crystal planes (111), (2 0 0), and (22 0) confirm the presence of Cu (JCPDS card no. 04–0836)(J. Cao et al., 2017a). The XRD pattern of the FTO substrate represents the typical diffraction peaks at 27°, 35°, 39°, 52°, 55°, 62°, 67°, and 79°of the FTO conductive glass substrate, which are assigned to tetragonal SnO_2 (JCPDS card no. 41-1445) Cu/MoS_2/FTO (Fluorine doped tin oxide) film (JCPDS No. 01-077-0452) has been used instead of Cu /MoS_2 /NF film for XRD analysis due to the high background signal of Ni generated by NF(Guo et al., 2020).

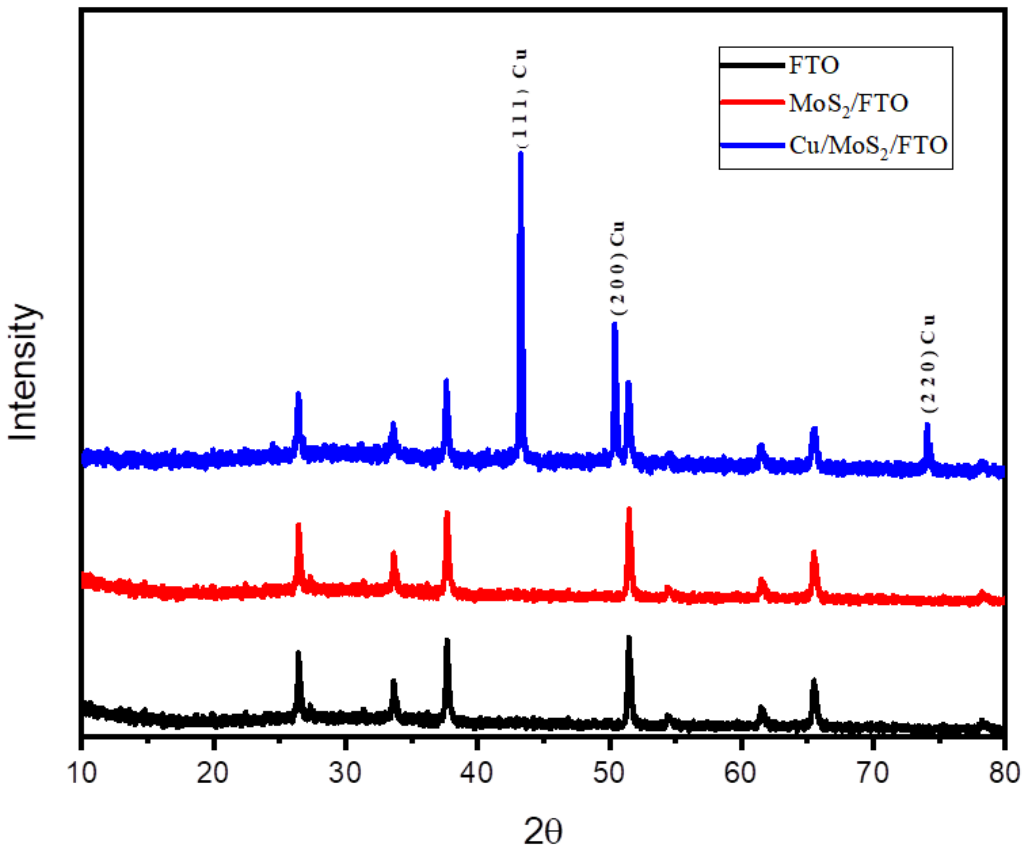

FIGURE8: XRD spectrum of bare FTO, MoS_2 /FTO and 100 s Cu/MoS_2 NPs.

4.1.2. HRTEM and SAED Analysis

High-Resolution transmission electron microscopy (HRTEM) images in (Figure 9a) revealed an interplanar spacing of 0.25 nm, which is consistent with the interplanar distance of the Cu (111) crystallographic plane, which is consistent with the XRD results (Figure 8).The selected area electron diffraction (SAED) in (Figure 9b),pattern of Cu/MoS_2 NSs exhibited the appearance of a ring pattern with regular spots in(Figure 9b). However, the regular ring pattern could be attributed to the presence of crystalline Cu NPs;the lattice fringes with spacing values of 0.25nm, 0.2271 nm, 0.1261 nm can be assigned to the (1 1 1), (2 0 0) and (2 2 0), planes of Cu respectively,are in good agreement with the XRD pattern(J. Cao et al., 2017a).

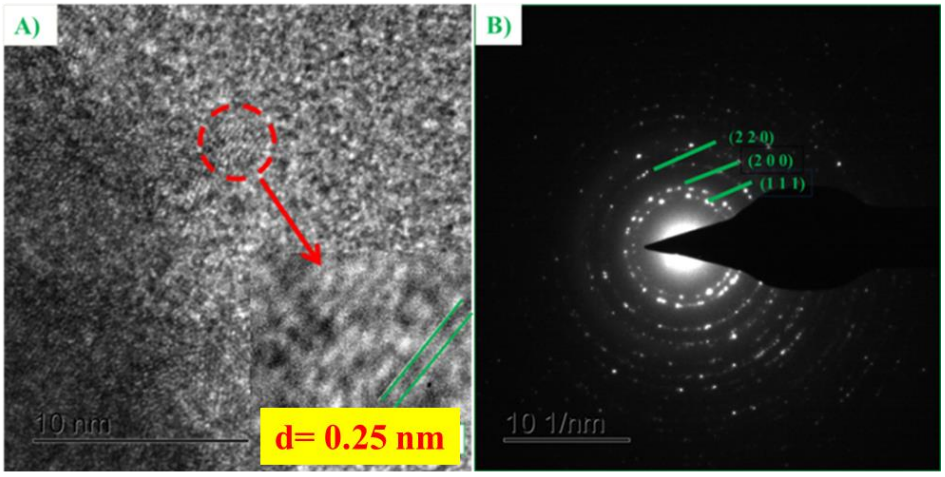

FIGURE9:(a) HRTEM images and (b) SAED images of 100s Cu/MoS_2nanostructures

4.1.3. SEM Analysis

The SEM morphology of single MoS_2 shows a smooth sheet, (Figure 10a). This can lead to a small in the surface area and active sites available for catalysis, which can negatively affect the catalytic activity. On the other hand, when MoS_2 is coated by Cu, it also shows a spherical shape, and it is distributed uniformly on the surface as shown on (Figure 10b). This indicates that Cu has played a crucial role in dispersing the MoS_2 particles on the substrate, leading to an increase in the surface area and active sites available for catalysis. This can significantly improve the catalytic activity of Cu/MoS_2.

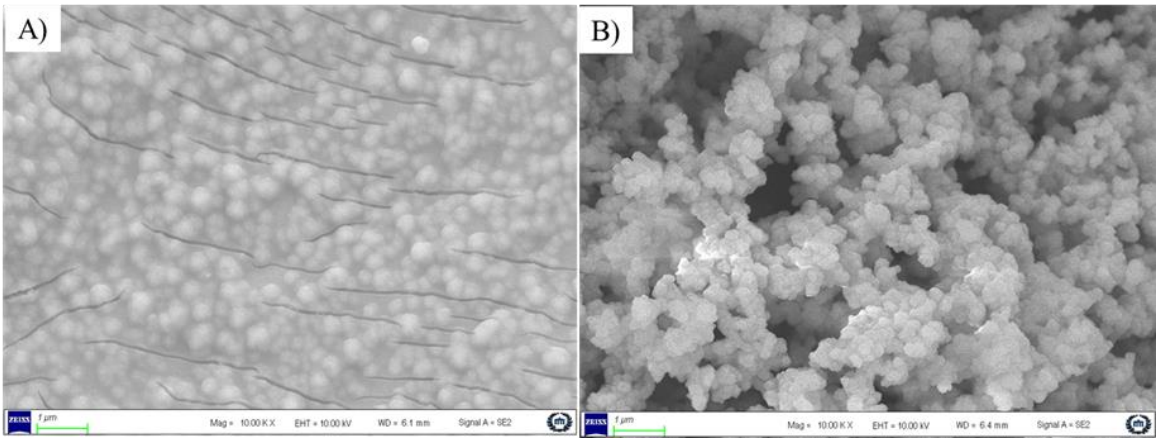

FIGURE10: SEM images of (a) MoS_2, (b) 100s Cu/MoS_2 NPs

4.1.4. TEM and Elemental Mapping Analysis

To further study the detailed microstructure of the as-prepared products, the Cu/MoS_2were scratched from the NF and examined by TEM. The TEM micrographs of100sCu/MoS_2illustrated in Figure 11 a ,which exhibited very finely grained Cu NPs with

spherical shapes which confirm with the SEM image of100s Cu/MoS_2in (Figure 10b).The elemental mapping data provides additional information about the distribution of these elements on the sample surface. The map shows in (Figure 11 b and c) that the Cu nanoparticles are distributed on all over the areas uniformly, with high concentrations of Cu appearing as bright spots on the map. Although, the Mo and S elements appear to be more evenly distributed across the surface, suggesting that the MoS_2 layer is still present and intact despite the presence of Cu. The EDS analysis shown in (Figure 11) confirms the presence of Mo, Cu, S, O and Ni in the sample. Ni is from NF, Moreover, the air contact results in the surface oxidation of Cu/MoS_2, which could be responsible for the peaks of oxygen (Ilyas, Raziq, Ali, Zada, Ilyas, Shaha, Wang, et al., 2021).

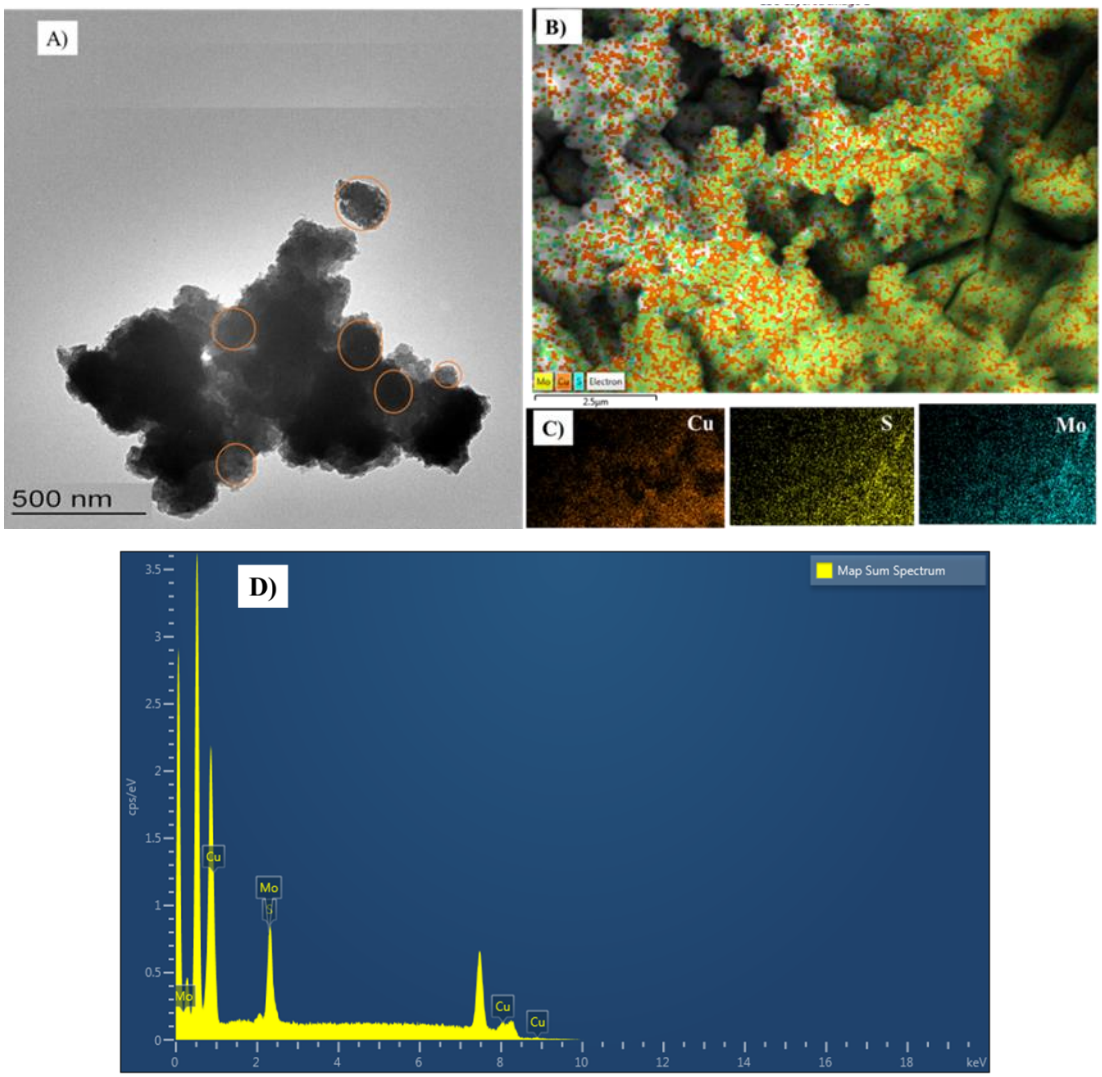

FIGURE11:(a) TEM images,(b and c) the corresponding elemental mapping and (d)SEM-EDS spectrum of 100s Cu/MoS_2

4.2. HER Catalytic Performance

The electrochemical performance of as-synthesized samples was evaluated in three electrode system synthesized materials (MoS_2,Cu/MoS_2) were used directly as HER working electrodes, platinum wire as counter electrode and Ag/AgCl as reference electrode The behavior of all the test sample catalysts against HER was in alkaline medium (1M KOH), with a scan rate of 2.0 mV/s. Frist when optimizing the catalytic activity of MoS_2 for hydrogen evolution reaction (HER), varied the deposition time of MoS_2 at a constant concentration (7mM) and applied potential (-1V) . Based on the cyclic voltammetry (CV) and linear sweep voltammetry (LSV) results shown on (Appendix Figure 2 (a and b)), shows that the MoS_2 deposited at 200 seconds exhibited better HER performance compared to the MoS_2 deposited at 100s,300 and 500 seconds. The CV and LSV results showed that the MoS_2 deposited at 200 seconds had a larger area under the HER peak and a lower overpotential than the MoS_2deposited at 300 and 500 seconds.

The larger area under the HER peak indicates a higher catalytic activity towards HER, while the lower overpotential indicates a more efficient HER process(Choudhury et al., 2021). The decreased HER performance of the MoS_2 deposited at 300 and 500 seconds compared to the MoS_2 deposited at 200 seconds can be attributed to the mass loading of MoS_2 on the electrode surface. High mass loading of the catalyst on the electrode, not all the surfaces of the catalyst can participate in the electrochemical reactions. Because not all the surface can be wetted by the electrolyte, especially for the region far from the interface of the electrolyte and the surface of the casted catalyst layer on the electrode (Yu et al., 2021).For the deposition Cu amount in the host of MoS_2-materials to be tuned, the time of deposition varied from 60s to 120s (60s, 80s, 100s, and 120s) at 0.1M concentration of the "Cu" precursor (($Cu(SO_4)_2.5H_2O$).

Largest CV curve area suggesting a highest specific capacity (Electro-catalytic activity) (Choudhury et al., 2021).LargestCV curve area was observed on the electrodes in which Cu NPs coated on MoS_2, when compared with single MoS_2 electrode as shown in (Figure 12). Among all electrode 100 s Cu/MoS_2has largest area ,due toelectro-catalytic activity MoS_2 increases with combination of Cu due toincrease the conductivity and improve the HER performance, this is because the Cu NPs can act as electron donors, providing electrons to the MoS_2.This transfer of electrons can promote the catalytic activity of both

materials, leading to a greater overall catalytic activity than either material alone ,also the obtained hybrid contains a large number of active HER catalytic sites due to the abundance of accessible edges resulting from the small size and irregular shape of MoS_2. Coating of copper not only improved the electrical conductivity of the catalyst but also further enhanced the catalytic activity by a synergistic effect with nano-sized MoS_2 (J. Cao et al., 2017a).However the hybrid contains a large number of active sites due to the abundance of accessible edges resulting from the spherical shape of CuNPs.

However, at 120 s deposition time of Cu NPs decreases the area of CV curve, due to overloaded Cu NPs inhibit the hydrogen/electron transfer reaction and offset the beneficial effect of mechanical strain on the electrochemical activity of the MoS_2NPstoward the HER due to poor in-plane alignment and high charge transfer resistance(Lee et al., 2014).CV by comparison, it can be found that the integral area of the bare NF electrode is quite small, indicating that the contribution of NF to the total capacity of 100s Cu/MoS_2/NF electrode is small.

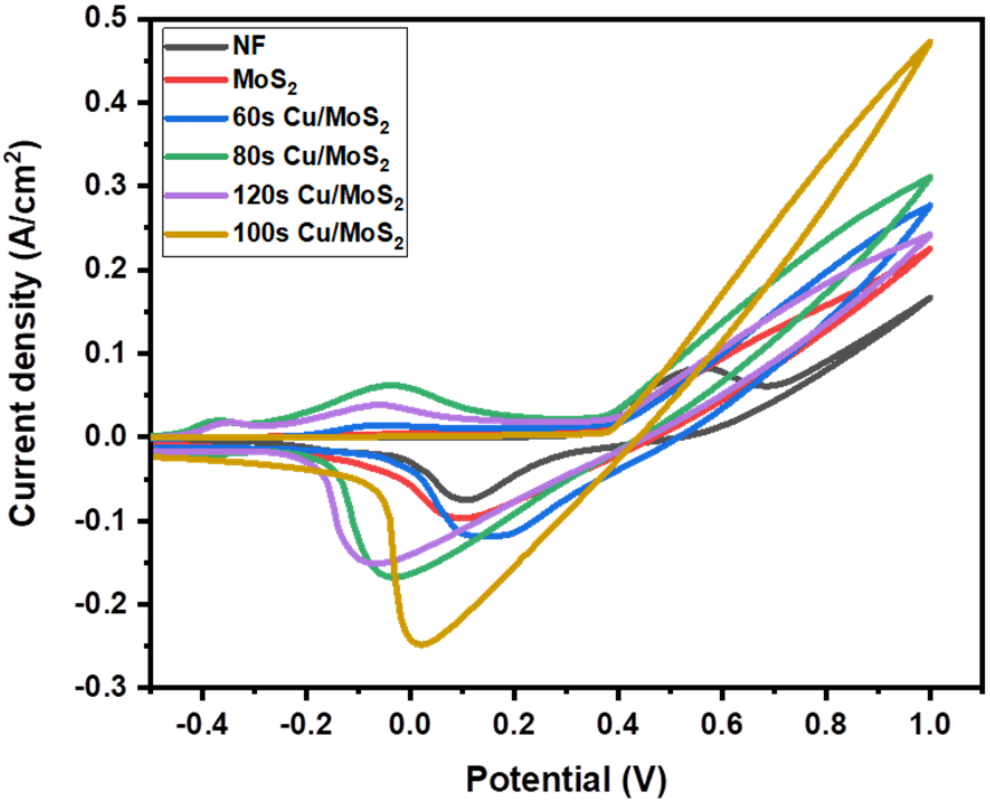

FIGURE12**:**CV curves of NF, MoS_2,and Cu/MoS_2 s recorded at a scan rate of 50 mV s^{-1}.

As shown LSV result in (Figure 13a), to produce 10 mA/cm^2 current density, NF requires −0.378 V,whereas MoS_2needs −0.258V and 100s Cu/MoS_2 need only −0.149V vs RHE which can reduce ~1.736-times than MoS_2-nanomaterial at an 10mAcm^{-2}.a clear cathodic shift in the onset potential observed after successful combination of Cu with MoS_2 this indicate that the combination of "Cu" with MoS_2-Nanomaterial essentially improve the electrocatalytic performance of MoS_2nanomaterial . Also (Figure 13b) shows clear Overpotential comparison and then 100s Cu/MoS_2 has small overpotential. Furthermore, the high hydrogen evolution reaction activity of 100s Cu/MoS_2 compares favorably with many previously reported MoS_2 based for Cu/MoS_2/NF electrocatalysts, as shown in (Table 2).

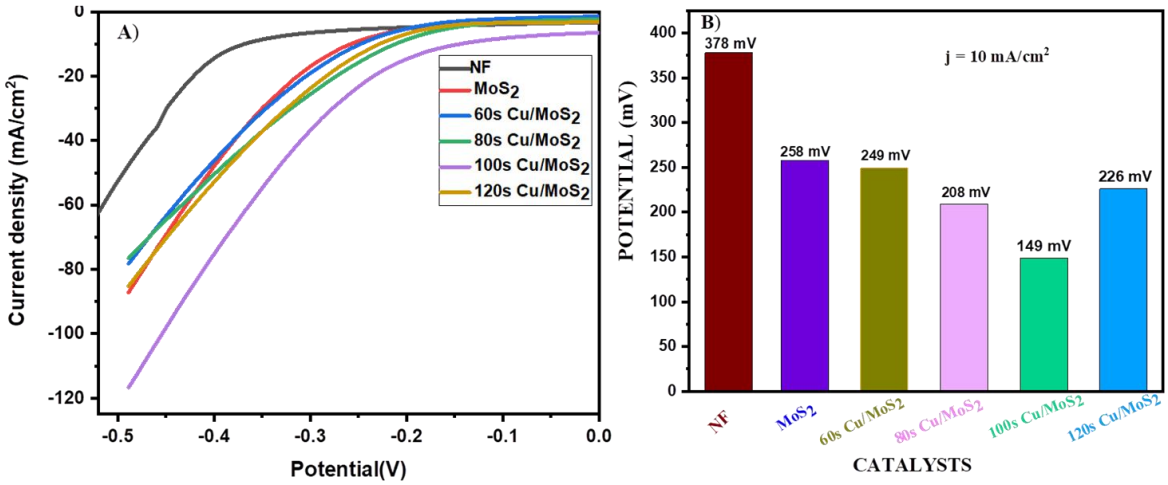

FIGURE13: (a) LSV polarization curves at a scan rate of 2 mV s^{-1}, (b) Overpotential comparison.

Table 1: Comparison of the electrocatalytic activity of the as-prepared Cu/MoS_2 (current density of 10 mA cm^{-2}) Nanomaterial toward HER with previously reported MoS_2 based catalysts.

Prepared Sample	**Electro lyte**	**Over-pote ntial (mV)**	**Synthesis Method**	**Ref**
Cu|MoS_2	KOH	149	ElectrodepositionMethod	This work
MWCNTs@C u@MoS_2	H_2SO_4	146	Solvothermal Method	(F. Li, Li, et al., 2015)

MoS2|Cu	KOH	160	Etching Method	(Ilyas, Raziq, Ali, Zada, Ilyas, Shaha, Wang, et al., 2021)
Ag-Ag_2S/MoS_2	H_2SO_4	150	Microwave-assisted technique.	(Sharma et al., 2021)
Etched MoS_2	H_2SO_4	316	One-step microwave-assisted method.	(J. Cao et al., 2017a)
MoS_2 Quantum Dot	H_2SO_4	190	Hydrothermal Method	8(Han et al., 2020)
MoS_2NTs array	H_2SO_4	296	Electrophoretic deposition	(Pataniya & Sumesh, 2022)
Cu-MoS_2- SV	H_2SO_4	197	Chemical etching method	3(Liu et al., 2023)
Cu_9S_5@MoS_2	KOH	146	Chemical vapor deposition (CVD)	(Z. Zhang et al., 2021)(Z. Zhang et al., 2021)
Cu-MoS_2/rGO	H_2SO_4	126	Hydrothermal Method	(F. Li, Zhang, et al., 2015)

The Tafel slope is a parameter used in electrochemistry to describe the reaction kinetics of an electrochemical reaction. It depicts how the current responds sensitively to an overpotential. It is derived from the polarization curve as a plot of the logarithm of current density (log(j)) versus η(Gicha et al., 2021). A lower Tafel slope value indicates faster reaction kinetics, while a higher tafel slope value indicates slower reaction kinetics. The Tafel slope is typically calculated using the Tafel equation, which relates the overpotential (η) to the exchange current density (a) and the Tafel slope (b): $\eta = b\log J + a$ (Sharma et al., 2021).It has been revealed that for a Tafel RDS (Rate DetarmaningStep) the slope is 29 mV/dec, whereas for the Heyrovsky and Volmer RDS, the slopes are 39 and 118 mV/dec. respectively(Briefs & Materials, n.d.). As shown in (Figure 14)Tafel slopes of 100sCu|MoS_2around 117 mV/decand relatively small than the other which areVolmer - Heyrovsky with the reaction mechanism.

$H_2O + e^- + * \rightarrow H^* + OH^-$ (Volmer reaction)

$H^* + H_2O + e^- \rightarrow H_2 + OH^- + *$(Heyrovsky reaction)

where, *is active site .This indicating that HER is controlled by the first electron transfer step (Volmer step), which is governed by the barrier of the electrochemical water dissociation.

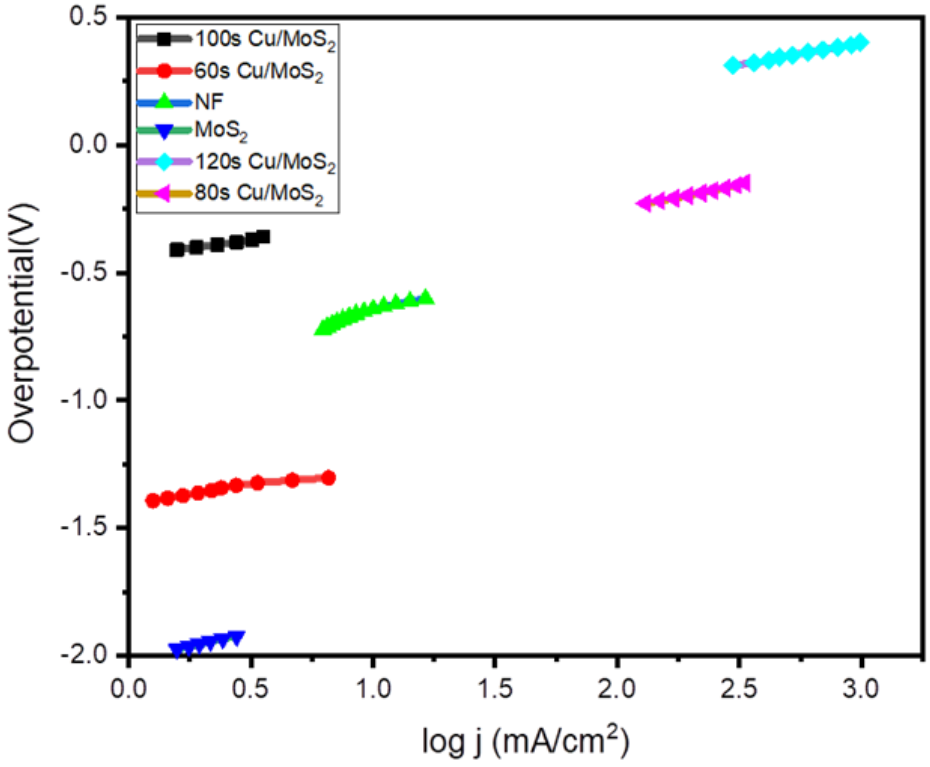

FIGURE 14:Tafel curve of various Cu/MoS_2NS carried out under a constant current density of 10 mA cm^{-2}.

Cyclic voltammetry (CV) is a useful technique to determine the electrochemically active surface area (Sharma et al., 2021).The CV measurements were conducted at various scan rates ranging from 20 to 120 mV s^{-1} in the potential window of −0.3 to −0.2 V *Vs* Ag/AgCl in 1 MKOH, as shown in (Figure 15). Double-layer capacitance (C_{dl}) values are calculated from the slope of the graph of current density Vs Scan rateare0.36,0.8,0.96,1.12,1.26and 4.8µF for NF,MoS_2,60sCu/MoS_2,80sCu/MoS_2,120sCu/$MoS_2$and 100sCu/MoS_2respectively shown in(Figure 16). The C_{dl} values are normalized by CS (specific capacitance) to find out the ECSA. The C_{dl}can be further converted into ECSA using the specific capacitance value for a standard with $1cm^2$ of real surface area (Connor et al., 2020).The specific capacitance for a flat surface isnormally between 0.02 - 0.06 mF cm^{-2}. For the purpose of this study, we use a specific capacitance of 0.04 mF cm^{-2}, which is a typical value for a

metal electrode in aqueous 1M KOH solution based on typical reported values (Duan et al., 2016).

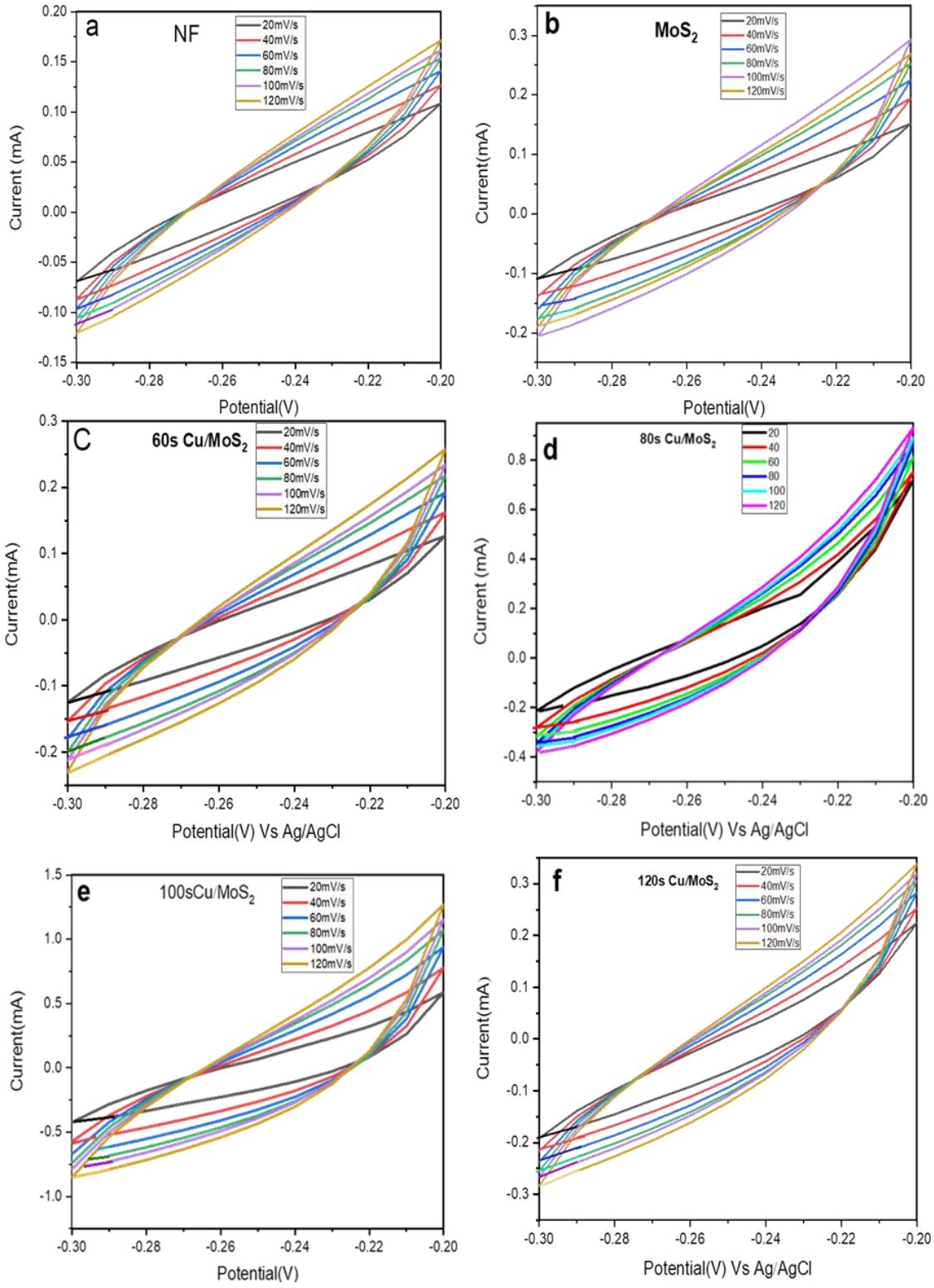

FIGURE15**:** Double layer capacitance measurements with scan rates at 20, 40, 60, 80, 100 and 120 mV/s in the region of – 0.3 to –0.2 V vs. Ag/AgCl for Cu/MoS_2/NF.

For the purpose of this study, we use a specific capacitance of 0.04 mF cm^{-2}, which is a typical value for a metal electrode in aqueous 1M KOH solution based on typical reported values (Duan et al., 2016). The calculated ECSA values for NF,MoS_2, 60sCu/$MoS_2$80sCu/MoS_2 120sCu/$MoS_2$and 100sCu/MoS_2- are0.009, 0.02,0.024 0.028, 0.0315 and 0.121 cm^2 , respectively,. The enhanced double-layer capacitance and ECSA reflect the higher electrocatalytic activity of 100sCu/MoS_2 compared to MoS_2.Roughness factor (Rf) is another parameter to judge the electrocatalytic activity of an electrocatalyst. R_f(active site per unit surface area)values are evaluated from the normalization of ECSA with the geometric surface areas ($1cm^2$)(Briefs & Materials, n.d.). The highest R_f value is determined for 100sCu/MoS_2, which is 0.121, and it is comparatively higher than that of others.

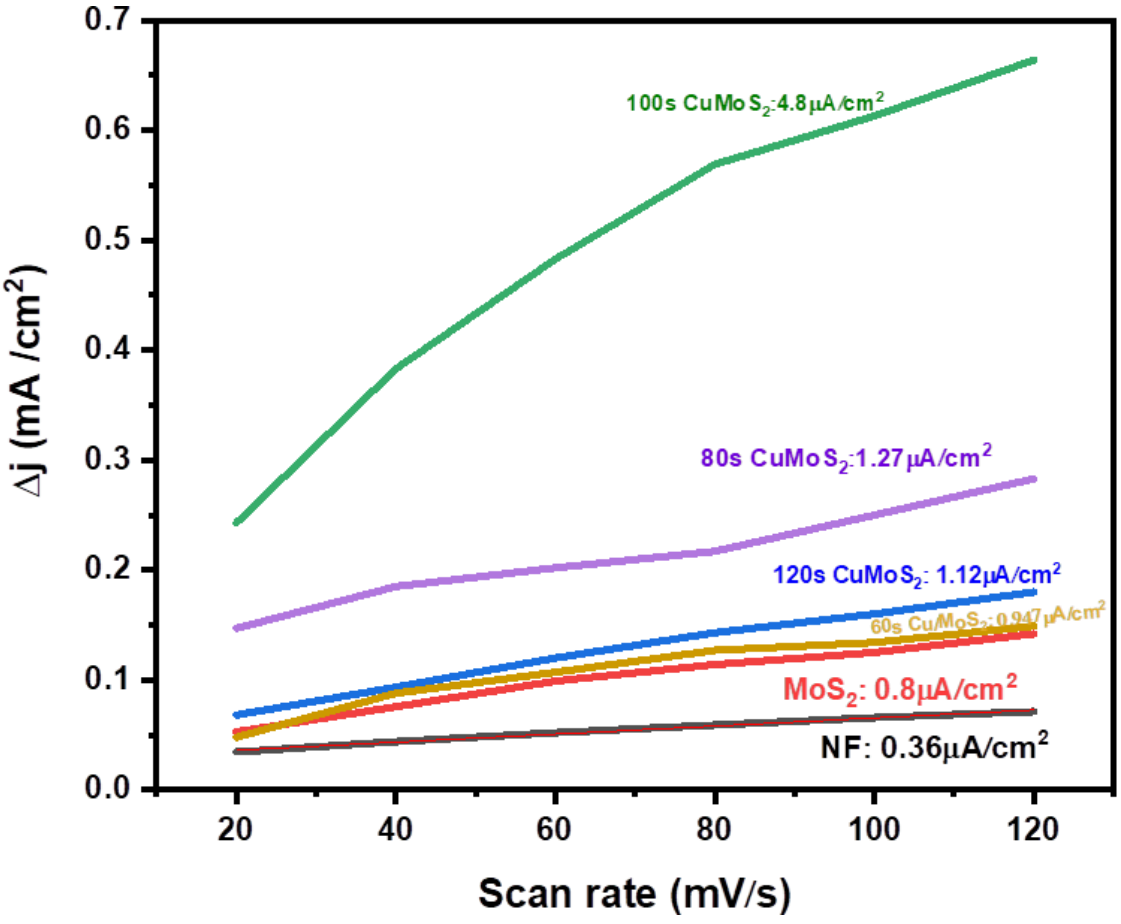

FIGURE 16: Capacitive current differences ($\Delta j = janode — jcathode$) at -0.25 V *vs*Ag/AgCl.

Turnover frequency (TOF) is another quantitative parameter used for evaluating an electrocatalyst at defined overpotential. The TOF of catalyst can be defined as the number

of moles of O_2/H_2 evolved per unit time(Anantharaj et al., 2016). TOF for HER was calculated with the following equation

$$TOF = \frac{|J| A}{2F.n}$$

Where |J| ($A \cdot cm^{-2}$) is the current density at a fixed voltage during the LSV measurement, A is the geometric area of the working electrode (1 cm^2), F is the Faraday constant (96485 $C \cdot mol^{-1}$), and n is the number of active sites.The number of active sites n is proportional to the charge Q, which can be calculated from the obtained CV curve by integrating. Therefore, active sites could be obtained from the following equation:

$$n = \frac{Q}{2F} = \frac{I.t}{2F} = \frac{I.V/u}{2F} = \frac{S}{2F.u}$$

Where S is integrated effective reduction area, I is the current (A), V is the voltage (V), u is the scan rate(Queiroz, 1997).The surface-active site concentrations were calculated from the reduction region of CV curves measured at 50 mV/s as shown in (Figure 17) and are found to be 2.1×10^{-6}atoms cm^{-2} , 2.8×10^{-6} atoms cm^{-2}, 3.4 $\times10^{-6}$ atoms cm^{-2} ,3.95×10^{-6}atoms cm^{-2} , $3.83\times10^{-6}$and.5.2×10^{-6} atoms cm-^{2} active component NF,MoS_2,60sCu/MoS_2,80s Cu/MoS_2, 120sCu/MoS_2, and 100sCu/MoS_2respectively. The addition of more cupper nanomaterial (Cu) to molybdenum disulfide (MoS_2) results in a slight increase in the concentrations number of active sites. The calculated TOF for 100sCu/MoS_2found to be 22 s^{-1} at 240 mV, which is higher than those of NF(12.5 s^{-1}), MoS_2(14 s^{-1}), 60sCu/MoS_2(16 s^{-1}),80s Cu/MoS_2 (19 s^{-1}),120s Cu/MoS_2(18.4 s^{-1}), indicating the superior intrinsic HER activity of 100s Cu/MoS_2

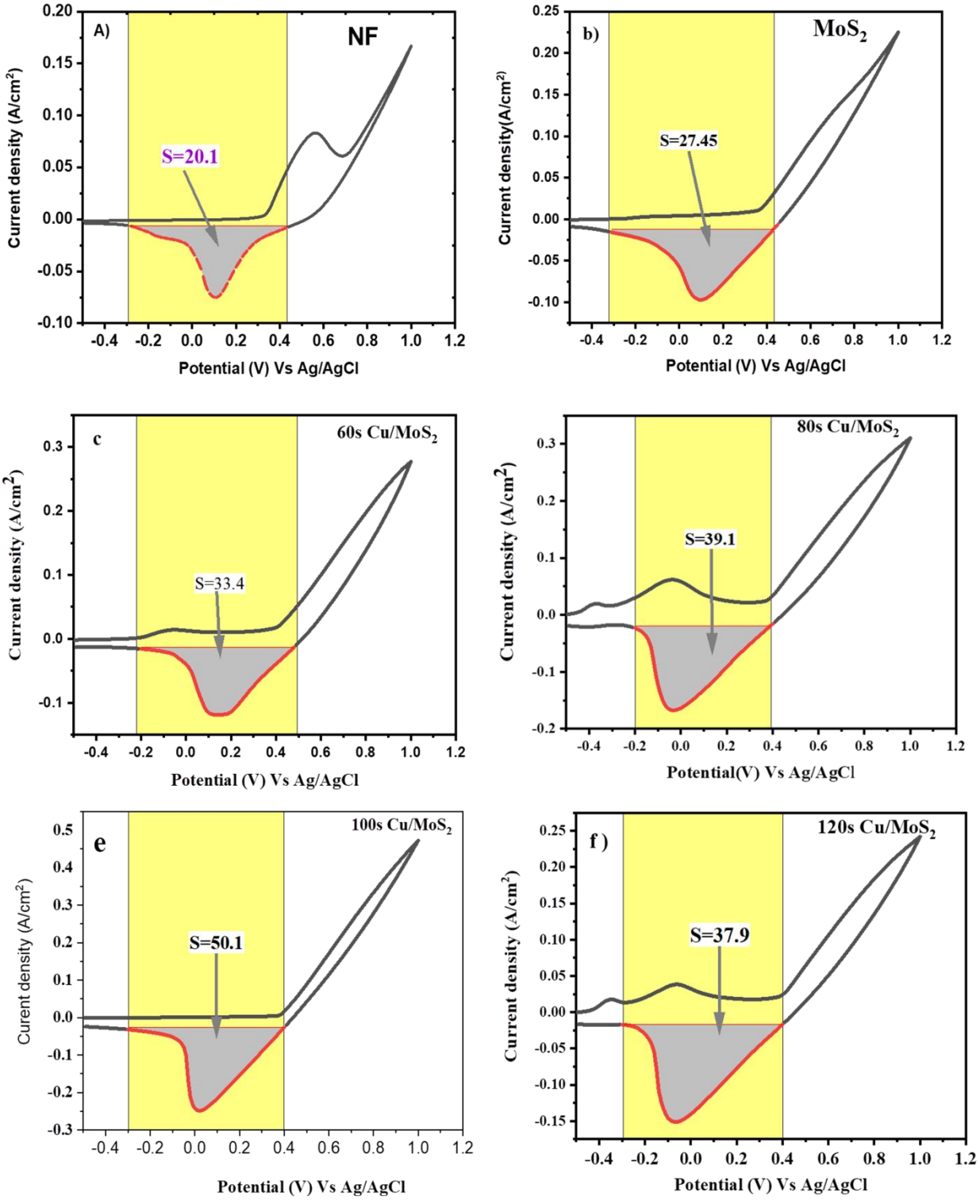

FIGURE 17: The reduction region of CV curves of all synthesized nanostructures' measured at a scan rate of 50 mV s-1.

Electrochemical impedance spectroscopy (EIS) was utilized to investigate the kinetics of the electrode at the electrolyte/electrode interface. A Nyquist plot was constructed with the

real impedance component (Z') on the x-axis and the imaginary component (-Z'') on the y-axis, and fitted with equivalent electrical circuits to quantitatively obtain device properties(Aguedo et al., 2020). The transfer of charge between the electrolyte and the electrocatalyst is a crucial factor that affects the efficiency of the HER process. The EIS analysis helps to determine the solution resistance as well as charge transfer resistance develops due to the charge transport in the interface of the electrocatalyst and electrolyte, where a lower value represents a faster rate of charge transfer(Sharma et al., 2021). The results depicted on(Figure18)indicate that 100s Cu/MoS_2 has a smaller R_{ct} value of 2.704 Ω, comparedMoS_2(16.9 Ω), and bare NF (25.7 Ω) indicating a more rapid charge transfer rate that is beneficial for an efficient HER process. This suggests that 100s Cu|MoS_2 is a more effective electrocatalyst for the HER process compared to the other materials studied. In summary, EIS is a valuable technique for investigating the electrochemical properties of electrocatalysts, providing insights into charge transfer kinetics, reaction mechanisms, and material performance under different conditions.

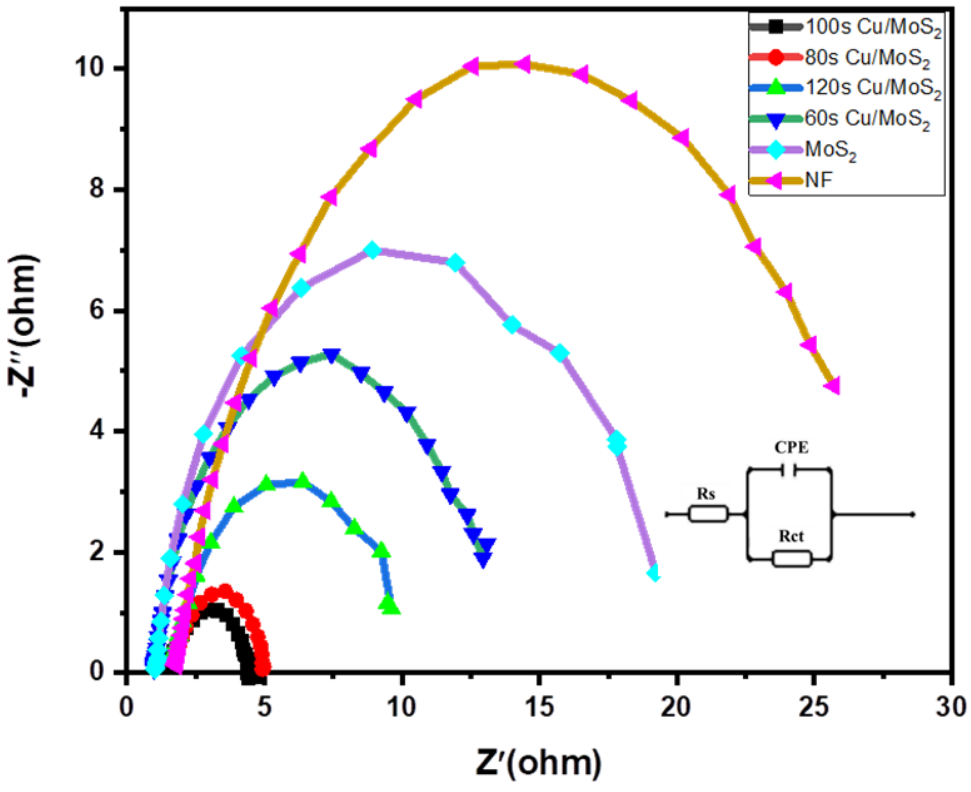

FIGURE18: Nyquist plots of Cu/MoS_2 carried out under a constant -149 mV Vs RHE of and equivalent electrical circuit inset.

The stability of a electrode can be evaluated by performing chronoamperometry, which involves applying a constant potential to the electrode and measuring the resulting current over time. In this case the 100s Cu/MoS_2 electrode produced a constant current density of 10 mA/cm^2 for a continuous 24-hour period show in (Figure 19), suggests that the electrode is stable and has good electrocatalytic activity for the reaction being studied. This is a positive indication of the electrode's stability and suggests that it may be suitable for long-term.

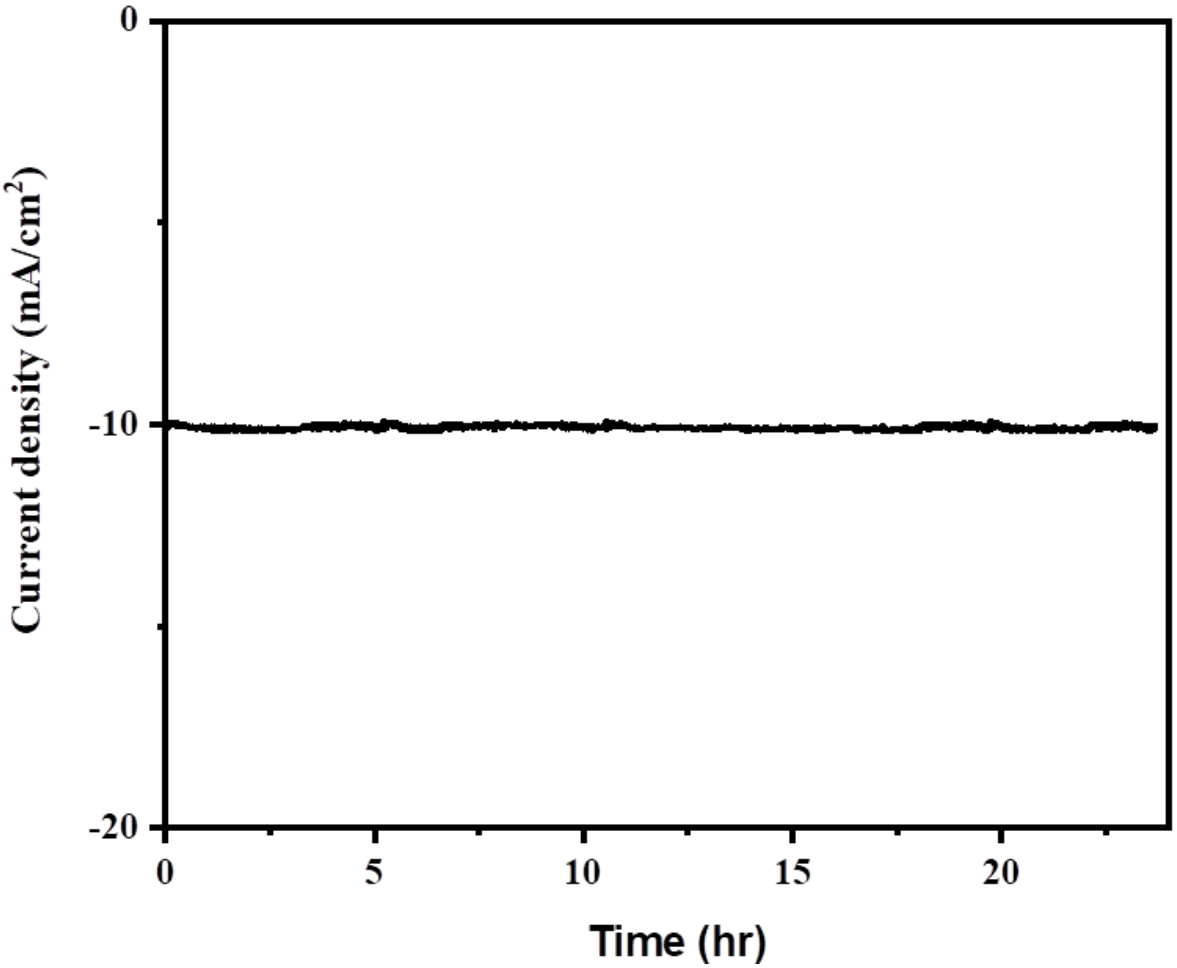

FIGURE19:Long-term stability test of 100 s Cu/MoS_2 carried out under a constant applied potential -149 mV Vs RHE

5. CONCLUSION AND RECOMMENDATION

5. 1 Conclusion

In conclusion, the development of efficient and cost-effective catalysts for the hydrogen evolution reaction (HER) is crucial for the practical application of HER water splitting. The limitations of MoS_2-based catalysts, including their low electrical conductivity and limited active sites on their surface, have hindered their widespread use in HER catalysis. Therefore, there is a need for new and effective synthesis methods and modifications to the MoS_2 substrate to overcome these limitations and improve the performance of MoS_2-based catalysts in HER catalysis.This study investigated the effectiveness of the electric field-assisted synthesis method for producing highly dispersed Cu/MoS_2 catalysts with improved catalytic activity for the HER. The Cu-MoS_2 catalysts synthesized using this method exhibited significantly improved catalytic activity and reduced overpotential compared to bare MoS_2 catalysts. The Cu nanoparticles deposited on the MoS_2 surface served as active sites for the HER and improved the electrical conductivity of the MoS_2 substrate, which facilitated electron transfer during the HER.The findings of this study highlight the potential of the electric field-assisted synthesis method and modifications to the MoS_2 substrate in improving the performance of MoS_2-based catalysts in HER catalysis. Further research in this area is needed to optimize these methods and understand their mechanisms to enable their practical application in various HER-related technologies. Overall, this study contributes to the development of efficient and cost-effective catalysts for the HER and advances the progress towards a sustainable hydrogen economy.

5.2. Recommendations

For the future study, there are a few recommendations on the computational simulations such as DFT to calculate adsorption free energies and mechanisms of Cu/MoS_2 nanomaterial that will give full information on active sites, which increases the catalytic activity. Furthermore, there are recommendations on the application of Cu/$MoS_2$for OER in order to compare the performance of it to HER and for supercapacitors.

REFERENCES

Aguedo, J., Lorencova, L., Barath, M., Farkas, P., & Tkac, J. (2020). Electrochemical impedance spectroscopy on 2d nanomaterial mxene modified interfaces: Application as a characterization and transducing tool. *Chemosensors*, *8*(4), 1–21. https://doi.org/10.3390/chemosensors8040127

Akram, H., Mateos-Pedrero, C., Gallegos-Suárez, E., Guerrero-Ruíz, A., Chafik, T., & Rodríguez-Ramos, I. (2014). Effect of electrolytes nature and concentration on the morphology and structure of MoS 2 nanomaterials prepared using one-pot solvothermal method. *Applied Surface Science*, *307*, 319–326. https://doi.org/10.1016/j.apsusc.2014.04.034

Alonso-Vante, N., Roldán, C. A. C., de Guadalupe González Huerta, R., Sánchez, G. R., & Robledo, A. M. (2019). Fundamentals of Electrocatalyst Materials and Interfacial Characterization. In *Fundamentals of Electrocatalyst Materials and Interfacial Characterization*. https://doi.org/10.1002/9781119460510

Anantharaj, S., Ede, S. R., Sakthikumar, K., Karthick, K., Mishra, S., & Kundu, S. (2016). Recent Trends and Perspectives in Electrochemical Water Splitting with an Emphasis on Sulfide, Selenide, and Phosphide Catalysts of Fe, Co, and Ni: A Review. *ACS Catalysis*, *6*(12), 8069–8097. https://doi.org/10.1021/acscatal.6b02479

Anh Ho, T., Kim, E., Yang, H., Joe, J., Hyeok Park, J., & Shin, H. (2021). Metal-Assisted Efficient Nanotubular Electrocatalyst of MoS2 for Hydrogen Production. *ChemCatChem*, *13*(14), 3237–3246. https://doi.org/10.1002/cctc.202100504

Apak, S., Atay, E., & Tuncer, G. (2017). Renewable hydrogen energy and energy efficiency in Turkey in the 21st century. *International Journal of Hydrogen Energy*, *42*(4), 2446–2452. https://doi.org/10.1016/j.ijhydene.2016.05.043

Bhat, K. S., & Nagaraja, H. S. (2021). Recent trends and insights in nickel chalcogenide nanostructures for water-splitting reactions. *Materials Research Innovations*, *25*(1), 29–52. https://doi.org/10.1080/14328917.2019.1703523

Briefs, S., & Materials, I. N. (n.d.). *Aneeya Kumar Samantara Satyajit Ratha*.

Briefs, S., & Materials, I. N. (2018). *Aneeya K. Samantara Satyajit Ratha*.

https://books.google.co.uk/books?hl=en&lr=&id=dfVADwAAQBAJ&oi=fnd&pg=PR5&dq=Aneeya+K.+Samantara+Satyajit+Ratha+materials+development&ots=v5UOewLdnC&sig=n8TXALS8quiE6cLC7v7g-xO5WpQ#v=onepage&q=Aneeya K. Samantara Satyajit Ratha materials development&f=fals

Cao, H., Bai, Z., Li, Y., Xiao, Z., Zhang, X., & Li, G. (2020). Solvothermal Synthesis of Defect-Rich Mixed 1T-2H MoS2Nanoflowers for Enhanced Hydrodesulfurization. *ACS Sustainable Chemistry and Engineering*, *8*(19), 7343–7352. https://doi.org/10.1021/acssuschemeng.0c00736

Cao, J., Zhou, J., Zhang, Y., & Liu, X. (2017a). A facile one-step fabrication of a novel Cu/MoS2 nano-assembled structure for enhanced hydrogen evolution reaction performance. *RSC Advances*, *7*(42), 25867–25871. https://doi.org/10.1039/c7ra01605k

Cao, J., Zhou, J., Zhang, Y., & Liu, X. (2017b). *RSC Advances nano-assembled structure for enhanced hydrogen*. 25867–25871. https://doi.org/10.1039/c7ra01605k

Choudhury, B. J., Roy, K., & Moholkar, V. S. (2021). Improvement of Supercapacitor Performance through Enhanced Interfacial Interactions Induced by Sonication. *Industrial and Engineering Chemistry Research*, *60*(20), 7611–7623. https://doi.org/10.1021/acs.iecr.1c00279

Connor, P., Schuch, J., Kaiser, B., & Jaegermann, W. (2020). The Determination of Electrochemical Active Surface Area and Specific Capacity Revisited for the System MnOx as an Oxygen Evolution Catalyst. *Zeitschrift Fur Physikalische Chemie*, *234*(5), 979–994. https://doi.org/10.1515/zpch-2019-1514

Duan, J., Chen, S., Vasileff, A., & Qiao, S. Z. (2016). Anion and Cation Modulation in Metal Compounds for Bifunctional Overall Water Splitting. *ACS Nano*, *10*(9), 8738–8745. https://doi.org/10.1021/acsnano.6b04252

Edwards, P. P., Kuznetsov, V. L., & David, W. I. F. (2007). Hydrogen energy. *Philosophical Transactions of the Royal Society A: Mathematical, Physical and Engineering Sciences*, *365*(1853), 1043–1056. https://doi.org/10.1098/rsta.2006.1965

Gicha, B. B., Tufa, L. T., Kang, S., Goddati, M., Bekele, E. T., & Lee, J. (2021). Transition metal-based 2d layered double hydroxide nanosheets: Design strategies and

applications in oxygen evolution reaction. *Nanomaterials*, *11*(6). https://doi.org/10.3390/nano11061388

Gudal, C. C., Pan, U. N., Paudel, D. R., Kandel, M. R., Kim, N. H., & Lee, J. H. (2022). *Bifunctional P - Intercalated and Doped Metallic (1T)-Copper Molybdenum Sul fi de Ultrathin 2D-Nanosheets with Enlarged Interlayers for E ffi cient Overall Water Splitting*. https://doi.org/10.1021/acsami.2c00278

Guo, M., Song, S., Zhang, S., Yan, Y., Zhan, K., Yang, J., & Zhao, B. (2020). Fe-Doped Ni-Co Phosphide Nanoplates with Planar Defects as an Efficient Bifunctional Electrocatalyst for Overall Water Splitting. *ACS Sustainable Chemistry and Engineering*, *8*(19), 7436–7444. https://doi.org/10.1021/acssuschemeng.0c01467

Gupta, D., Chauhan, V., & Kumar, R. (2020). A comprehensive review on synthesis and applications of molybdenum disulfide (MoS2) material: Past and recent developments. *Inorganic Chemistry Communications*, *121*(August), 108200. https://doi.org/10.1016/j.inoche.2020.108200

Han, D., Luo, Z., Li, Y., Gao, N., Ge, J., Liu, C., & Xing, W. (2020). Synergistic engineering of MoS2 via dual-metal doping strategy towards hydrogen evolution reaction. *Applied Surface Science*, *529*(July), 147117. https://doi.org/10.1016/j.apsusc.2020.147117

Herbaut, M., Siaj, M., & Claverie, J. P. (2021). Nanomaterials-Based Water Splitting: How Far Are We from a Sustainable Solution? *ACS Applied Nano Materials*, *4*(2), 907–910. https://doi.org/10.1021/acsanm.1c00246

Huang, J., Jiang, Y., An, T., & Cao, M. (2020). Increasing the active sites and intrinsic activity of transition metal chalcogenide electrocatalysts for enhanced water splitting. *Journal of Materials Chemistry A*, *8*(48), 25465–25498. https://doi.org/10.1039/d0ta08802a

Ilyas, T., Raziq, F., Ali, S., Zada, A., Ilyas, N., Shaha, R., & Wang, Y. (2021). Materials & Design Facile synthesis of MoS 2 / Cu as trifunctional catalyst for electrochemical overall water splitting and photocatalytic CO 2 conversion. *Materials & Design*, *204*, 109674. https://doi.org/10.1016/j.matdes.2021.109674

Ilyas, T., Raziq, F., Ali, S., Zada, A., Ilyas, N., Shaha, R., Wang, Y., & Qiao, L. (2021).

Facile synthesis of MoS2/Cu as trifunctional catalyst for electrochemical overall water splitting and photocatalytic CO2 conversion. *Materials and Design*, *204*, 109674. https://doi.org/10.1016/j.matdes.2021.109674

Krishnan, U., Kaur, M., Singh, K., Kumar, M., & Kumar, A. (2019). A synoptic review of MoS 2 : Synthesis to applications. *Superlattices and Microstructures*, *128*, 274–297. https://doi.org/10.1016/j.spmi.2019.02.005

Lee, J. H., Jang, W. S., Han, S. W., & Baik, H. K. (2014). Efficient hydrogen evolution by mechanically strained MoS2 nanosheets. *Langmuir*, *30*(32), 9866–9873. https://doi.org/10.1021/la501349k

Li, F., Li, J., Lin, X., Li, X., Fang, Y., Jiao, L., An, X., Fu, Y., Jin, J., & Li, R. (2015). Designed synthesis of multi-walled carbon nanotubes@Cu@MoS2 hybrid as advanced electrocatalyst for highly efficient hydrogen evolution reaction. *Journal of Power Sources*, *300*, 301–308. https://doi.org/10.1016/j.jpowsour.2015.09.084

Li, F., Zhang, L., Li, J., Lin, X., Li, X., & Fang, Y. (2015). Synthesis of Cu e MoS 2 / rGO hybrid as non-noble metal electrocatalysts for the hydrogen evolution reaction. *Journal of Power Sources*, *292*, 15–22. https://doi.org/10.1016/j.jpowsour.2015.04.173

Li, X. L., Li, T. C., Huang, S., Zhang, J., Pam, M. E., & Yang, H. Y. (2020). Controllable Synthesis of Two-Dimensional Molybdenum Disulfide (MoS2) for Energy-Storage Applications. *ChemSusChem*, *13*(6), 1379–1391. https://doi.org/10.1002/cssc.201902706

Li, Y., Wang, H., Xie, L., Liang, Y., Hong, G., & Dai, H. (2011). MoS2 nanoparticles grown on graphene: An advanced catalyst for the hydrogen evolution reaction. *Journal of the American Chemical Society*, *133*(19), 7296–7299. https://doi.org/10.1021/ja201269b

Liu, Y., Guan, S., Du, X., Chen, Y., Yang, Y., Chen, K., Zheng, Z., Wang, X., Shen, X., Hu, C., & Li, X. (2023). S-Vacancy Defect and Transition-Metal Atom Doping to Trigger Hydrogen Evolution of Two-Dimensional MoS 2 . *Energy & Fuels*. https://doi.org/10.1021/acs.energyfuels.2c03942

Liu, Y., Luo, X., Zhou, C., Du, S., Zhen, D., Chen, B., Li, J., Wu, Q., Iru, Y., & Chen, D. (2020). A modulated electronic state strategy designed to integrate active HER and

OER components as hybrid heterostructures for efficient overall water splitting. *Applied Catalysis B: Environmental*, *260*(September 2019). https://doi.org/10.1016/j.apcatb.2019.118197

Lu, Q., Yu, Y., Ma, Q., Chen, B., & Zhang, H. (2016). 2D Transition-Metal-Dichalcogenide-Nanosheet-Based Composites for Photocatalytic and Electrocatalytic Hydrogen Evolution Reactions. *Advanced Materials*, *28*(10), 1917–1933. https://doi.org/10.1002/adma.201503270

Pang, L., Barras, A., Zhang, Y., Amin, M. A., Addad, A., Szunerits, S., & Boukherroub, R. (2019). CoO Promoted the Catalytic Activity of Nitrogen-Doped MoS2 Supported on Carbon Fibers for Overall Water Splitting [Research-article]. *ACS Applied Materials and Interfaces*, *11*(35), 31889–31898. https://doi.org/10.1021/acsami.9b09112

Pataniya, P. M., & Sumesh, C. K. (2022). MoS2 nanosheets on Cu-foil for rapid electrocatalytic hydrogen evolution reaction. *Journal of Electroanalytical Chemistry*, *912*(December 2021), 116270. https://doi.org/10.1016/j.jelechem.2022.116270

Queiroz, N. (1997). Supporting Information Supporting Information. *Aldenderfer, Mark S., Craig, Nathan M., Speakman, Robert Jeff, and Popelka-Filcoff, Rachel S.*, *2*(1), 1–5.

Quy, V. H. V., Vijayakumar, E., Ho, P., Park, J. H., Rajesh, J. A., Kwon, J. M., Chae, J., Kim, J. H., Kang, S. H., & Ahn, K. S. (2018). Electrodeposited MoS2 as electrocatalytic counter electrode for quantum dot- and dye-sensitized solar cells. *Electrochimica Acta*, *260*, 716–725. https://doi.org/10.1016/j.electacta.2017.12.023

Rastogi, P. K., Sarkar, S., & Mandler, D. (2017). Ionic strength induced electrodeposition of two-dimensional layered MoS2 nanosheets. *Applied Materials Today*, *8*, 44–53. https://doi.org/10.1016/j.apmt.2017.04.004

Rosen, M. A., & Koohi-Fayegh, S. (2016). The prospects for hydrogen as an energy carrier: an overview of hydrogen energy and hydrogen energy systems. *Energy, Ecology and Environment*, *1*(1), 10–29. https://doi.org/10.1007/s40974-016-0005-z

Samantara, A. K., & Ratha, S. (2019). Mechanism and Key Parameters for Catalyst Evaluation. *SpringerBriefs in Materials*, 11–29. https://doi.org/10.1007/978-3-030-24861-1_3

Sharma, M. D., Mahala, C., Modak, B., Pande, S., & Basu, M. (2021). Doping of MoS2by “cu” and “v”: An Efficient Strategy for the Enhancement of Hydrogen Evolution Activity. *Langmuir*, *37*(16), 4847–4858. https://doi.org/10.1021/acs.langmuir.1c00036

Sun, J., Li, X., Guo, W., Zhao, M., Fan, X., Dong, Y., Xu, C., Deng, J., & Fu, Y. (2017). Synthesis methods of two-dimensional MoS2: A brief review. *Crystals*, *7*(7), 1–11. https://doi.org/10.3390/cryst7070198

Sun, J., & Meng, X. (2021). Modulating the Electronic Properties of MoS2Nanosheets for Electrochemical Hydrogen Production: A Review. *ACS Applied Nano Materials*, *4*(11), 11413–11427. https://doi.org/10.1021/acsanm.1c02832

Tang, Q., & Jiang, D. E. (2016). Mechanism of hydrogen evolution reaction on 1T-MoS2 from first principles. *ACS Catalysis*, *6*(8), 4953–4961. https://doi.org/10.1021/acscatal.6b01211

Tiwari, A. P., Novak, T. G., Bu, X., Ho, J. C., & Jeon, S. (2018). Layered ternary and quaternary transition metal chalcogenide based catalysts for water splitting. *Catalysts*, *8*(11). https://doi.org/10.3390/catal8110551

Toh, R. J., Sofer, Z., Luxa, J., Sedmidubský, D., & Pumera, M. (2017). 3R phase of MoS2 and WS2 outperforms the corresponding 2H phase for hydrogen evolution. *Chemical Communications*, *53*(21), 3054–3057. https://doi.org/10.1039/c6cc09952a

Wan, L., Wang, Y., Zhang, Y., Du, C., Chen, J., Xie, M., Tian, Z., & Zhang, W. (2021). Designing FeCoP@NiCoP heterostructured nanosheets with superior electrochemical performance for hybrid supercapacitors. *Journal of Power Sources*, *506*(June), 230096. https://doi.org/10.1016/j.jpowsour.2021.230096

Wang, F., Shifa, T. A., Zhan, X., Huang, Y., Liu, K., Cheng, Z., Jiang, C., & He, J. (2015). Recent advances in transition-metal dichalcogenide based nanomaterials for water splitting. *Nanoscale*, *7*(47), 19764–19788. https://doi.org/10.1039/c5nr06718a

Wang, J., Yue, X., Yang, Y., Sirisomboonchai, S., Wang, P., Ma, X., Abudula, A., &Guan, G. (2020). Earth-abundant transition-metal-based bifunctional catalysts for overall electrochemical water splitting: A review. *Journal of Alloys and Compounds*, *819*, 153346. https://doi.org/10.1016/j.jallcom.2019.153346

Wang, Z., Li, Q., Xu, H., Dahl-Petersen, C., Yang, Q., Cheng, D., Cao, D., Besenbacher, F., Lauritsen, J. V., Helveg, S., & Dong, M. (2018). Controllable etching of MoS2 basal planes for enhanced hydrogen evolution through the formation of active edge sites. *Nano Energy*, *49*(May), 634–643. https://doi.org/10.1016/j.nanoen.2018.04.067

Wu, W., Wei, C., Shen, Y., & Chu, S. (2019). *Beijing Synchrotron Radiation Facility , Institute of High Energy Physics , Chinese Academy of SC*. https://doi.org/10.1016/j.apcatb.2019.03.053

Yin, Z., Liu, X., Chen, S., Ma, T., & Li, Y. (2022). Interface Engineering and Anion Engineering of Mo-Based Heterogeneous Electrocatalysts for Hydrogen Evolution Reaction. *Energy and Environmental Materials*, 1–18. https://doi.org/10.1002/eem2.12310

Yu, L., Sun, S., Li, H., & Xu, Z. J. (2021). Effects of catalyst mass loading on electrocatalytic activity: An example of oxygen evolution reaction. *Fundamental Research*, *1*(4), 448–452. https://doi.org/10.1016/j.fmre.2021.06.006

Yu, L., Zhou, H., Sun, J., Qin, F., Luo, D., Xie, L., Yu, F., Bao, J., Li, Y., Yu, Y., Chen, S., & Ren, Z. (2017). Hierarchical Cu@CoFe layered double hydroxide core-shell nanoarchitectures as bifunctional electrocatalysts for efficient overall water splitting. *Nano Energy*, *41*, 327–336. https://doi.org/10.1016/j.nanoen.2017.09.045

Zhang, Y., Xue, L., Liang, C., Chen, Y., Liu, J., Shen, C., Li, Q., Duan, Y., Yao, L., Zhang, H., Cai, Y., Tan, C., & Luo, Z. (2021). Two-dimensional metallic MoS2-amorphous CoNi(OH)2 nanocomposite for enhanced electrochemical water splitting in alkaline solutions. *Applied Surface Science*, *561*(April), 1–8. https://doi.org/10.1016/j.apsusc.2021.150079

Zhang, Z., Zhu, H., Hao, J., Lu, S., Duan, F., Xu, F., & Du, M. (2021). One-dimensional, space-confined, solid-phase growth of the Cu9S5@MoS2 core–shell heterostructure for electrocatalytic hydrogen evolution. *Journal of Colloid and Interface Science*, *595*, 88–97. https://doi.org/10.1016/j.jcis.2021.03.097

Zhao, J., Wang, J., Chen, Z., Ju, J., Han, X., & Deng, Y. (2021). Metal chalcogenides: An emerging material for electrocatalysis. *APL Materials*, *9*(5). https://doi.org/10.1063/5.0049772

Zou, X., & Zhang, Y. (2015a). Chem Soc Rev for water splitting †. *Chemical Society Reviews*. https://doi.org/10.1039/C4CS00448E

Zou, X., & Zhang, Y. (2015b). Noble metal-free hydrogen evolution catalysts for water splitting. *Chemical Society Reviews*, *44*(15), 5148–5180. https://doi.org/10.1039/c4cs00448e

APPENDIX

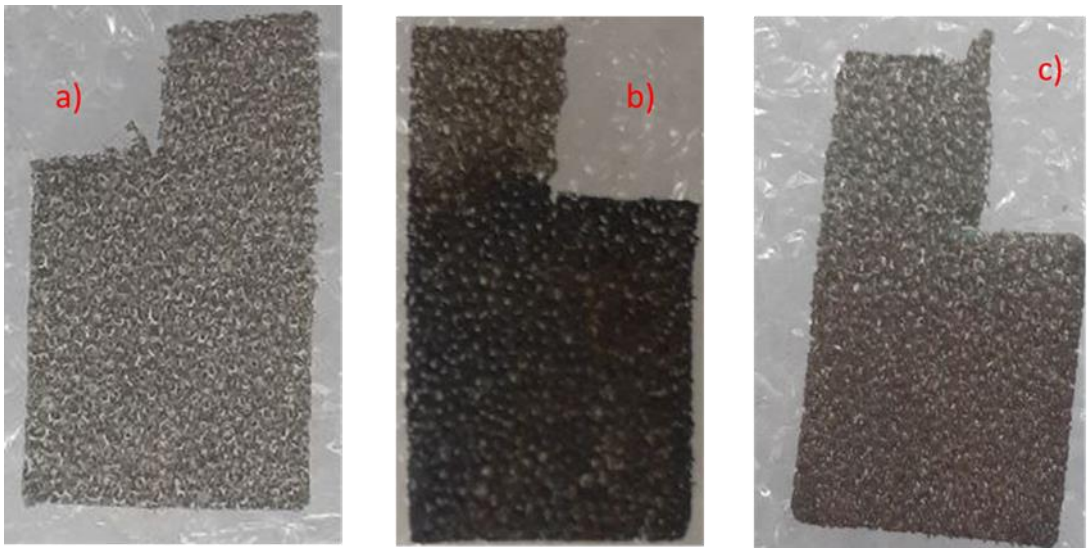

Apendix Figure 1. Digital photographs of (a) bare NF, (b) MoS_2, and (c) Cu/MoS_2NSs

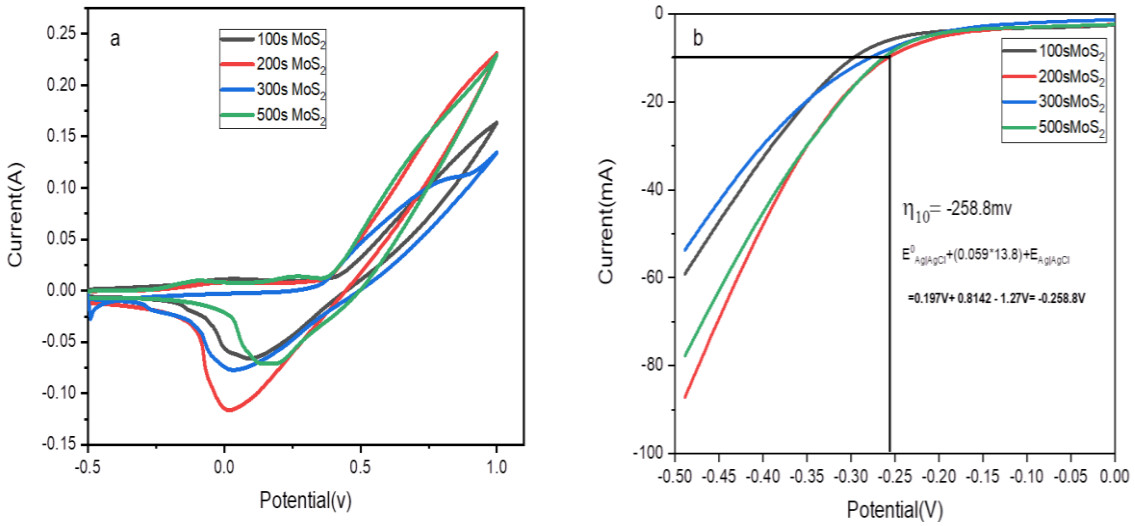

Appendix Figure 2. (a) CV curves recorded at a scan rate of 50 mV s^{-1} , Electrochemical performance of various MoS_2.NS electrodes carried out under a constant current density of 10 mA cm^{-2} in 1 M KOH aqueous solution. (b) HER polarization curves